Organic Geochemistry
November 2011, Volume 173, Pages 104484 (18p.)
https://doi.org/10.1016/j.orggeochem.2022.104484
https://archimer.ifremer.fr/doc/00789/90051/

Fatty acid biomarkers as indicators of organic matter origin and processes in recent turbidites: The case of the terminal lobe complex of the Congo deep-sea fan

Pruski Audrey M. [1, *], Stetten Elsa [1, 2], Huguet Arnaud [3], Vétion Gilles [1], Wang Haolin [1], Senyarich Claire [1], Baudin François [2]

[1] Sorbonne Université, CNRS, Laboratoire d'Ecogéochimie des Environnements Benthiques, LECOB, F-66650, Banyuls-sur-Mer, France
[2] Sorbonne Université, CNRS, UMR 7193, ISTeP, F-75005, Paris, France
[3] Sorbonne Université, CNRS, EPHE, UMR 7619, METIS, F-75005, Paris, France

* Corresponding author : Audrey M. Pruski, email address ; audrey.pruski@obs-banyuls.fr

Abstract :

The Congo River is connected to its submarine canyon and supplies large quantities of terrestrial organic carbon via powerful turbiditic currents down to the Congo deep-sea fan. We investigated sediment cores from the terminal lobe complex of the Congo deep-sea fan (~ 750 km offshore, ~ 5000 m water depth), in order to assess the value of fatty acid biomarkers as indicators of organic matter (OM) origin and processes affecting its distribution and preservation in recent turbidites. Sediments from the Congo deep-sea fan are enriched in fatty acids compared to the surrounding abyssal plains and their composition closely resembles that of sediments recovered in the Congo River. Long chain fatty acid (LCFA) biomarkers in conjunction with the branched vs isoprenoid tetraether index (BIT) show that organic matter mostly originates from soil erosion and continental higher plants. This material has undergone limited reprocessing during transit certainly due to tight interactions with mineral particles and rapid transfer. The presence of phytoplankton biomarkers at the entrance of the terminal lobe area highlights that inputs of fresh organic matter, albeit limited, can reach the lobe complex. By combining fatty acid profiles and geochemical proxies in a multivariate analysis, we highlight that OM degradation is mostly limited to the oxic layer, and that fine soil-derived particles and the coarser higher plant detritus display distinct depositional dynamics. Finally, LCFA are remarkably well preserved under anoxic conditions at different time scales, in recent turbidites deposited during the last century and those deposited several thousand years ago.

Graphical abstract

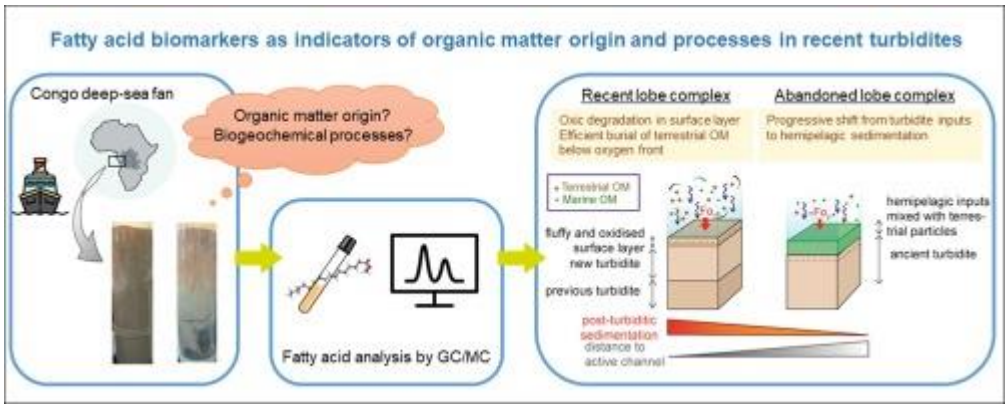

Highlights

► Fatty acids in Congo lobe sediments are mainly of terrestrial origin. ► Soil OM is distributed homogenously and plant debris heterogeneously. ► Small amounts of biomarkers from phytoplankton reach the terminal lobe complex. ► Oxic degradation is limited to the topmost surface sediments. ► Long chain fatty acids are preserved in turbidite deposits over millennia.

Keywords : Congo deep-sea fan, terminal lobe complex, turbidite deposition, fatty acid biomarkers, soil derived-organic matter, degradation, preservation

1. Introduction

What happens to terrestrial organic matter (OM) in the deep ocean is still an open question because of our limited knowledge of the biogeochemical transformations which occur during transport and after deposition on abyssal plains (Hedges et al., 1997; Benner, 2004; Burdige, 2005; Blair and Aller, 2012; Bianchi et al., 2014). The fate of terrestrially derived OM depends on many factors, among which its sources and inherent properties, physical protection mechanisms shielding labile components from microbial degradation, or aging processes occurring on the continental shelf and beyond (Mayer et al., 2004; Ding and Sun, 2005; Wakeham and Canuel, 2006; Dai et al., 2009; Bao et al., 2019). The depositional setting itself and the surrounding physicochemical conditions also constrain the fate of the deposited OM (Sun and Wakeham, 1994; Hedges and Keil, 1995; Hoefs et al., 2002; Wakeham and Canuel, 2006). Disentangling the contribution of all these factors on the cycling of OM in deep basins is thus challenging, as each environment is unique.

Due to the diversity of sources and complexity of the processes involved, combining bulk geochemical proxies and molecular markers is often necessary to get accurate insights into the origins of sedimentary OM and its diagenetic evolution (Prahl et al., 1997; Shi et al., 2001; Weijers et al., 2009). Ancient turbidites from the Madeira Abyssal Plain have provided geochemists with a natural laboratory to study the effects of long-term oxygen exposure (ca. 8000 years or more, Buckley and Cranston, 1988) on terrestrial OM preservation and lipid biomarker records (Prahl et al., 1997; Hoefs et al., 2002; Huguet et al., 2008). They found that up to 80% of the OM initially deposited was degraded in the oxic layer of the turbidites and that re-exposure to oxygen severally impacted the lipid biomarker content and composition. Yet, the drivers of OM degradation and the extent of lipid biomarker alteration in recent turbiditic deposits, as those observed in active submarine canyons remain largely unknown.

The Congo deep-sea fan is an ideal site to study the processes affecting the fate of recent

inputs of terrestrial OM in the deep-sea. The Congo River is the second largest exporter of terrestrial organic carbon (OC) to the world's ocean and delivers 14.4 Tg of OC per year to the equatorial Atlantic Ocean, of which 2 Tg is particulate organic carbon (POC) (Coynel et al., 2005). The submarine canyon of the Congo River extends across the entire continental shelf directly into the estuary, maintaining a constant connection between the African continent and a deep-sea channel-levee-lobe system (Heezen et al., 1964; Fig. 1). Long-lasting turbidity currents are frequently generated in the canyon and enable the rapid export of sediments along the meandering active channel downslope to the terminal lobe complex located ~ 750 km from the African coast at a depth of ~ 5000 m (Fig. 1; Savoye et al., 2009; Babonneau et al., 2010; Azpiroz-Zabala et al., 2017). This non-steady state depositional pattern characterised by high sedimentation rates and rapid burial is a key driver of the preservation of terrestrial organic carbon, because it tends to limit the exposure of the POC to oxygen in the water column (Hedges and Keil, 1995). Hence, in this remarkable depositional context, the terminal lobe complex of the Congo deep-sea fan represents the main present-day depocenter for the POC delivered by the Congo River (Stetten et al., 2015; Baudin et al., 2017a) and is a major carbon sink in the equatorial Atlantic Ocean (Rabouille et al., 2019; Baudin et al., 2020).

The suspended OM delivered by the Congo River is mainly composed of soil-derived mineral-associated OM, with increasing contribution of recently fixed rainforest vegetation and plant debris and decreasing contribution from phytoplankton during periods of elevated runoff (Spencer et al., 2012; Hemingway et al., 2017). Terrestrial OM is regarded as being relatively refractory, owing to the presence of lignocellulosic polymers in terrestrial plants, the formation of complex geomacromolecules during humification and the tight association of soil OM with the mineral matrix (Hedges and Oades, 1997). Therefore, the terrestrial OM transferred by turbidity currents to the terminal lobe complex of the Congo deep-sea fan

should have a high potential for preservation. The suspended sediment exported by the Congo River is characterised by higher loads of functionalised lipids (fatty acids and alcohols) relative to alkanes (Hemingway et al., 2016). Since fatty acids and alcohols degrade faster

than bulk OC and alkanes, their prevalence in the suspended sediments indicates they are sourced from local surface soils with limited exposure to diagenesis prior export (Hemingway et al., 2016). This also means that a pool of reactive OM is delivered by the Congo River to the Atlantic Ocean.

The current study focuses on fatty acids, a versatile class of lipid biomarkers commonly used to trace the sources and evolution of riverine OM in the land-ocean continuum (Bianchi and Canuel, 2011). Owing to the generally assumed sensitivity of fatty acids to diagenesis and degradation, these biomarkers are also ideal proxies to explore processes participating in OM alteration during transit and after deposition in the deep-sea fan. Using fatty acid biomarkers, their isotopic composition and the branched versus isoprenoid tetraether (BIT) index, a proxy of fluvially exported soil OM (Hopmans et al., 2004; Weijers et al., 2009), this study complements parallel investigations undertaken in the same area (Stetten et al., 2015; Baudin et al., 2017a, 2017b; Méjanelle et al., 2017; Pruski et al., 2017; Schnyder et al., 2017) and aims to provide new insights into: (1) the origins, (2) source to sink transformations, and (3) post-depositional processes affecting the OM in the terminal lobe complex of the Congo deep-sea fan.

To this end, we first identified the most likely biological sources of fatty acids in seven sediment cores collected in the terminal lobe complex. We then compared these records to terrestrial and marine end-members (sediments from the Congo River and marine suspended OM) in order to highlight compositional changes occurring during transit. We finally related fatty acid distribution and downcore evolution to the geochemical proxies reported here and in

earlier studies (Table 1). This multiproxy approach enables to address the general question: "Are fatty acids good indicators of OM sources and processes in recent turbidites?".

2. Material and methods

2.1. Environmental setting: The Congo deep-sea fan and the terminal lobe area

Marine productivity off the mouth of the Congo River ranges from 50 $gC.m^{-2}\ y^{-1}$ to 450 $gC.m^{-2}y^{-1}$ (Berger, 1989; Wenzhöfer and Glud, 2002). This marine productivity is sustained by strong coastal upwellings on either side of the Congo River estuary (Schneider et al., 1994; Schefuß et al., 2004) and by the river plume, which persists 800 km from the coast (Van Bennekom and Berger, 1984). Dissolved OM (< 0.7 µm) and a high proportion of fine POM (< 63 µm) are mainly exported through this turbid plume (Cadée, 1984) where they are widely recycled by microbial processes and extensive photo-degradation (Spencer et al., 2009), while the remaining (fine and coarse) POM is mainly exported by the Congo River canyon (Cadée, 1984).

The Congo deep-sea fan extends nearly 1000 km off the African coast and covers an estimated area of 330000 km^2 (Savoye et al., 2000). It is considered as one of the major deposition centres in the South Atlantic Ocean with 5.4×10^{13} t of OC accumulated since 34 Ma (Baudin et al., 2010). Turbidity currents triggered in the Congo canyon are funnelled in the unique and meandering active channel whose present-day length is 1135 km, and ultimately reach the terminal lobe complex (Fig. 1a; Babonneau et al., 2010).

The terminal lobe complex, which covers 2500 km^2 (less than 1% of the total area of the Congo deep-sea fan) (Rabouille et al., 2017) was explored during the Congolobe cruise (Rabouille, 2011). Five sites (A, F, C, B and E) corresponding to distinct geomorphological features were selected for the present study (Fig. 1b). Three sites are located along the active channel (A, F and C) (Fig. 1b; Rabouille et al., 2017). Site A is located at the entry of the lobe

complex and presents a well-pronounced channel-levee structure compared to site F, which is located 40 km downstream. Site C is located at the end of the feeding channel and represents the ultimate sink for turbidity currents. This site collects the dilute upper part of the turbidity

current (Dennielou et al., 2017); in the rest of this paper it is referred to as the terminal depocenter. Short-lived radionuclide activities (^{137}Cs and $^{210}Pb_{xs}$) in sediment cores from these three sites revealed that huge amounts of sediments have been deposited in the last century (0.5 cm.y^{-1} to 12 cm.y^{-1} Stetten et al., 2015; Rabouille et al., 2017). Site B is located ~15 km northeast of the active channel and remains exposed to turbidity current overflow (Bonnel, 2005; Dennielou et al., 2017). In contrast, site E is located ~40 km northward of site B in an older lobe complex and is completely disconnected from the active system since at least the Holocene as shown by the absence of caesium in sediments sampled at this site and by the dominant marine geochemical signature in the top ten centimetres (Stetten et al., 2015; Schnyder et al., 2017). This site has not been exposed to turbidity currents for ca. 4 000 years (Picot et al., 2016, 2019), and will thus be considered as abandoned.

2.2. Sampling

Seven sediment cores corresponding to 42 samples of sediments from the terminal lobe complex were analysed in this study (Fig. 1; see Supplementary Table S1 for coordinates of sampling sites). Sampling took place in December 2011 to January 2012 during the Congolobe oceanographic campaign (Rabouille, 2011). Short sediment cores were collected using a MUC 8/100 multicorer (Oktopus GmbH) and were rapidly sliced into 11 layers (0–0.5 cm; 0.5–1 cm; 1–2 cm; 2–3 cm; 3–5 cm; 5–7 cm; 7–10 cm; 10–13 cm; 13–16 cm; 16–19 cm; 19–22 cm). The layers were carefully homogenised, placed in Falcon tubes, and stored at –80 °C until analysis.

Five samples of suspended POM from the surface waters overlaying the study area were

also collected by filtering 10 L of seawater on pre-combusted glass fibre filters (45 mm Whatman GF/F). Our sampling was completed with 6 samples from the Malebo Pool floodplain wetlands near Kinshasa (donated by H. Talbot and B. Spencer). Organic matter

from the Malebo Pool is considered as a good reference for the terrestrial OM exported by the Congo River as limited compositional changes occur between this site and the head of the estuary (Spencer et al., 2012). The OM deposited in the Malebo Pool is representative of the soil OM eroded from the Congo watershed as well as some local production that occurs within the wetlands (Spencer-Jones et al., 2015). The samples were collected from two distinct depths (surface: 0–5 cm and subsurface: 5–15 cm) at 3 sites encompassing permanently flooded sediment, sediment inundated during high discharge months only and sediment from above the seasonal high-water point (Talbot et al., 2014). These samples will be referred in the text as permanently submerged, recently exposed and floodplain sediments.

2.3. Contextual geochemical and sedimentological properties

Bulk geochemical and sedimentological data for sediments from the distal lobe complex have been published previously: grain size, elemental composition and bulk stable carbon and nitrogen isotope values in Stetten et al. (2015), Rock-Eval signatures in Baudin et al. (2017b) and total hydrolysable amino acid composition in Pruski et al. (2017) for 34 of the 42 samples. These analyses were performed on aliquots of the same samples as those used in the present study allowing direct comparison.

Briefly, sediment grain size was assessed using a Malvern Mastersizer 2000 laser diffraction particle size analyser following treatment of wet sediments with HCl to remove carbonate. Total organic carbon content was measured on dried sediments using a high temperature combustion method (LECO IR 212 with an induction furnace HF-100, LECO Corporation) with correction for inorganic carbon content measured by carbonate-bomb

and/or a pyrolytic method (Baudin et al., 2015). Pyrolytic analyses were carried out using a Rock-Eval 6 Turbo device, operating in a mode devoted to recent sediments (Baudin et al., 2015). Among the parameters delivered by Rock-Eval analysis, the oxygen index (OI)

provides insights on the amount of oxygen relative to the amount of OC present in a sample and was selected for this study as a proxy of the oxidation state of the OM. Subsamples of freeze-dried sediments were pre-treated with 1N HCl to remove carbonates prior stable isotope analysis. C/N molar ratios, and stable isotope compositions of carbon and nitrogen were determined by on-line combustion of the decarbonated sediments on a Carlo Erba NC 2500 instrument connected to an Isoprime isotope ratio mass spectrometer (Stetten et al., 2015).

Total hydrolysable amino acids (THAA) were extracted from freeze-dried sediments by acid hydrolysis (hot 6N HCl, 24 h, 110 °C). After neutralisation with NaOH 6N, carbamates were produced from amino acids by alkylation with propyl-chloroformate in the presence of *n*-propanol and pyridine (Dettmer et al., 2012). Carbamates were recovered by liquid-liquid partition using iso-octane, purified and analysed on a gas chromatograph (CLARUS 580) fitted with a flame ionization detector (Perkin Elmer). The obtained mole percentages were used to calculate the degradation index (DI), which synthesises subtle changes in the amino acid composition linked with diagenesis into a univariate variable indicative of OM degradation state (Dauwe et al., 1999). As arginine does not produce stable carbamates, this amino acid was omitted from the DI calculation. In Dauwe's initial dataset, the DI varied from −2.2 for extensively degraded sediments to +1.5 for fresh algae, but more extreme values have been reported (Unger et al., 2005).

2.4. Lipid biomarker analysis

2.4.1. GDGT analysis and BIT index determination

Extractions for the glycerol dialkyl glycerol tetraether (GDGT) lipids were performed on the surface (0–1 cm layer) and deeper (19–22 cm) intervals of each core from the lobe complex according to the protocol described in Coffinet et al. (2014). Since limited amounts

of surface sediments were available, freeze-dried sediments from the two first horizons were pooled before extraction (0.5 g of the 0–0.5 cm layer and 0.5 g of the 0.5–1 cm layer), whereas 1 g of the 19–22 cm layer was weighed.

GDGT analysis was performed by high performance liquid chromatography–atmospheric pressure chemical ionization mass spectrometry (HPLC–ACPI-MS), with a Shimadzu LC-MS 2020. During elution, the proportion of hexane and isopropanol was modified by time steps in the conditions described in Coffinet et al. (2014). The injection volume was 10 µL. Semi-quantification of GDGTs was performed by comparing the integrated signal of the respective compound with the signal of a C_{46} synthesized internal standard (Huguet et al., 2006) assuming their response factors to be identical.

The branched vs isoprenoid tetraether (BIT) index, a proxy for fluvial input of soils, was calculated according to the equation proposed by Hopmans et al. (2004):

$$\mathrm{BIT} = \frac{(\mathrm{I} + \mathrm{II} + \mathrm{III})}{(\mathrm{I} + \mathrm{II} + \mathrm{III} + \mathrm{IV})}$$

where I, II, III are branched GDGTs and IV is crenarchaeol (refer to Hopmans et al. (2004) for the GDGT structures). The BIT index thus potentially ranges from 0 to 1, with high values indicating high soil input relative to marine production (see Table 1 for proxy interpretation). Triplicate injections of three samples indicated that the analytical error for the BIT was 0.01.

2.4.2. Fatty acid extraction and analysis

Fatty acid analyses were performed on the 11 layers of the cores from the site C channel and from the abandoned site E, on the surface, sub-surface, mid-layer and deeper horizons of all the other cores (0–0.5 cm; 0.5–1 cm; 5–7 cm and 19–22 cm) as well as on the marine and

terrestrial references. Aliquots of freeze-dried material (~1.5 g) were treated with a solution of methanol, sulphuric acid and chloroform (at 90 °C for 90 min) in the presence of an internal standard (nonadecanoic acid; $C_{19:0}$) and an antioxidant (butyl hydroxytoluene, Christie, 1993).

This direct acid transesterification protocol enables in one single step to extract the lipids, release the fatty acids and produce simultaneously the corresponding methyl esters (see Bourgeois et al., 2011 for the detailed procedure).

Fatty acid methyl esters (FAME) were dissolved in 50 µL of hexane prior to their analysis by gas chromatography and mass spectrometry (GC–MS; GC Varian 3900 coupled to a Saturn 2100T ion trap detector). FAME were separated on a capillary ZB wax column (30 m × 0.25 mm ID, 0.25 µm film thickness; Phenomenex) using helium at 1 mL min^{-1} and a specific temperature gradient (Bourgeois et al., 2011). The MS system was operated with electron impact ionization at 70 eV in full scan mode (scanning *m*/*z* 40–650 in a 1 s cycle). Based on the total ion chromatograms (TIC), FAME were identified by comparing their retention times with those of commercial FAME standards (Qualmix Fish Synthetic, Ladoran Fine Chemicals, INTERCHIM, France; Supelco 37, PUFA No. 1 and No. 3, SUPELCO France) and matching the mass spectra with the NIST library.

The quantifier ion of each analyte was extracted from the TIC and used for quantification. External calibration curves were then obtained from a series of dilutions of a quantitative standard mixture (Supelco 37) supplemented with four fatty acids ($C_{19:0}$, $C_{26:0}$, $C_{28:0}$ and $C_{30:0}$) and used to determine fatty acid concentrations. Repeatability of the analysis, determined by comparing relative standard deviations of 41 fatty acids in six different preparations of our standard solution, ranged from 1.0% to 5.4% with a mean value of 2.4%. Fatty acid concentrations initially expressed in µg per gram dry weight (µg g^{-1} dw) were normalised to the OC content of the respective sample (stated as mg g^{-1} OC).

Five fatty acid subgroups were defined for the study: short-chain saturated fatty acids

(SCFA; $C_{14:0}$–$C_{23:0}$), long chain saturated fatty acids (LCFA; $C_{24:0}$–$C_{30:0}$), monounsaturated fatty acids (MUFA; $C_{16:1\omega7}$, $C_{18:1\omega9\ cis}$, $C_{18:1\omega7}$, $C_{20:1\omega9}$), polyunsaturated fatty acids (PUFA; [illegible]), and bacterial fatty acids (BAFA; [illegible]

$aiC_{15:0}$, $iC_{16:0}$, $iC_{17:0}$, 3-OH-C_{12}, 3-OH-C_{14}). Source assignment of individual fatty acid was based on the literature (Table 1). Compound specific stable isotope analysis of fatty acids in sediments was further performed at the Center for Applied Isotope Studies (University of Georgia) to confirm their provenance (see the Supplementary material for detailed procedures).

The unsaturation index (UI), average chain length ($ACL_{16–30}$) and carbon preference index (CPI) of the fatty acids were calculated from the following formula (Claustre et al., 1992; Wiesenberg et al., 2010; Angst et al., 2016):

$UI = \sum(z_{n:x} \times x)$ where z_n is the relative amount of the fatty acids with n carbon atoms and x is the number of unsaturation

$ACL_{16-30} = \sum(z_n \times n)/\sum z_n$ where z_n is the relative amount of the fatty acids with n carbon atoms and n was 16 to 30 carbon atoms

$CPI = 0.5 \times \left[\frac{\sum C_{12-30}^{even}}{\sum C_{11-29}^{odd}} + \frac{\sum C_{12-30}^{even}}{\sum C_{13-31}^{odd}}\right]$; CPI was calculated for the entire, lower- and higher molecular weight ranges.

2.5. Statistical analyses and data treatment

Statistical analyses were performed using R software (3.6.3). Due to the non-normal distribution of most of the variables, non-parametric statistical analyses were used to examine relationships between variables (Spearman non-parametric test, ρ). p-values below 0.05 were considered statistically significant.

Unconstrained multivariate analyses were performed to explore relationships among sediment samples and to determine whether fatty acid profiles were related to the other

biogeochemical parameters. Sediment samples were associated with respect to their fatty acid profiles using hierarchical agglomerative clustering with the Bray-Curtis dissimilarity index and Ward's minimum variance linkage method. The agnes function of package "cluster" was used for clustering (Maechler et al., 2019) and the Bray-Curtis distances were square-rooted before applying Ward's algorithm. Variations in fatty acid distribution between sampling sites and sediment depths were visualised using non-metric multidimensional scaling (nMDS) based on a Bray-Curtis dissimilarity distance matrix (function metaMDS of package "vegan", Oksanen et al., 2016) as described by Wakeham et al. (2012). The resulting ordination plot displays samples defined by sites and sediment depths, and fatty acid distribution. The function envfit ("vegan" package) was used to overlay environmental factors (biogeochemical parameters) on the nMDS ordination and find significant correlations. Environmental factors were fitted in the ordination plot as vectors, whereby the arrow indicates the direction of the increasing gradient of the environmental variable and the length of the arrow is proportional to the correlation coefficient between the variable and the nMDS ordination. Fatty acid data were square root transformed prior to analysis to down-weight the contribution of very dominant fatty acids, while absolute numbers were used for all other variables.

3. Results

3.1. Contextual geochemical and sedimentological properties

Despite being collected in different morpho-sedimentary settings, the bulk properties of sediments from the recent lobe complex (sites A, F, C and B) were similar (Table 2). They were characterised by high OC contents (2.2–4.1%), highly negative $\delta^{13}C_{org}$ values around –26.5‰, $\delta^{15}N$ values ranging between 4.6 and 5.9, and high C/N ratios (14.0–22.5). In these sediments, OI values ranged from 244 to 324 mg CO_2 g^{-1} TOC, which indicates variable degrees of oxidation of the OM. The DI generally exhibited slightly negative values in the

oxic surface layers with a trend for higher values with depth, indicative of a lower degradation state. Sediments were composed of silt (70–79%) and clay (12–28%) with a minor and variable proportion of coarser material (0–16%).

The geochemical properties of sediments from the abandoned site (site E) enabled us to identify two distinct intervals. The top seven cm were characterised by low OC contents (0.7–0.9%), lower C/N ratios (11.0–11.7), higher $\delta^{13}C_{org}$ values (–23.9‰ to –22.8‰), higher OI values (up to 609 mg CO_2 g^{-1} OC) and lower DI values (around –1) indicative of a more advanced stage of degradation. In contrast, sediments in the deeper layers (7–22 cm) have increasing OC contents (from 1.2% to 2.8%), higher C/N ratios (12.3–15.9), lower $\delta^{13}C_{org}$ values (below –24.1‰), lower OI values (less than 270 mg CO_2 g^{-1} TOC) and higher DI values (–0.52 to +0.24). The changes of the geochemical properties across the sediment core are consistent with a major shift in the sources of the OM incorporated in the sediments, from degraded hemipelagic inputs to the top layers to less degraded terrestrial OM in deeper layers (Stetten et al., 2015).

3.2. GDGT-based proxy

GDGT analyses were performed on two sediment layers (0–1 cm and 19–22 cm). Relative abundances of GDGTs and concentrations in isoprenoid and branched GDGTs are reported in Supplementary Table S2. Branched GDGTs were more abundant than isoprenoid GDGTs, especially crenarchaeol, in almost all sediments resulting in high BIT index values (> 0.7, Table 3). In the present-day active lobe complex, BIT values displayed a narrow range (0.75–0.84) with lower values in surface sediments than in deeper ones (Table 3). One lower value (0.48), explained by the low abundance of branched GDGTs vs crenarchaeol, was obtained for the surface sediment at the abandoned site E, but the deeper layer had a BIT value of 0.76, similar to those measured in sediments from the active lobe complex. Crenarchaeol accounted

on average for 44% of the isoprenoid GDGTs with concentrations ranging from 17 to 134 µg g^{-1} OC.

3.3. Fatty acid composition and concentration in the terrestrial and marine references

The fatty acid composition of Congo River sediments collected on land and marine suspended POM recovered above the terminal lobe complex is presented in Fig. 2 (see Supplementary Table S3 for the detailed composition of the terrestrial and marine references). At the Malebo Pool, the recently exposed sediments were enriched in OC by a twofold factor in comparison to recently exposed and floodplain sediments, but OC-normalised fatty acid concentrations were similar and ranged in the upper horizon between 7.1 mg g^{-1} OC for the recently exposed sediments and 9.1 mg g^{-1} OC for the floodplain (Fig. 3). The fatty acid composition of the river sediments was characterised by high contributions of saturated fatty acids (SAFA: 55.6% to 70.7%) with a dominance of $C_{16:0}$, medium contributions of bacterial fatty acids (BAFA: 16.8% to 26.9%), and lower contributions of monounsaturated fatty acids (MUFA: 9.5% to 15.2%) and polyunsaturated fatty acids (PUFA: 0.5% to 8.4%) (Fig. 2). Among the SAFA, long chain fatty acids (LCFA) accounted for 16.4% to 28.9% of all fatty acids with the preponderance of $C_{24:0}$. MUFA $C_{18:1\omega9cis}$ and PUFA $C_{18:2\omega6cis}$ were abundant in river sediments, particularly in the surface layer from the floodplain with contributions of these two fatty acids reaching 9.8% and 8.1%, respectively (Supplementary Table S3).

Fatty acid concentrations of suspended POM ranged from 7.8 µg L^{-1} at site B to 94.2 µg L^{-1} at site A (Supplementary Table S3). Surface waters were characterised by the predominance of SAFA (47.1% to 66.7%), in particular $C_{16:0}$ and $C_{18:0}$ (Fig. 2). The suspended POM also contained MUFA (12.2% to 17.9%) and PUFA (9.2% to 30.5%), and small amounts of BAFA (3.3% to 5.3%). The surface water at site A stood out from the other samples because its fatty acid concentration was one order of magnitude higher. In addition,

this sample was enriched in PUFA (32.4%), with $C_{22:6\omega3}$ accounting for 21.8% of all fatty acids (Supplementary Table S3).

3.4. Fatty acid composition and concentrations in sediments from the terminal lobe complex

Sediments from the lobe complex contained approximately 1.5 times less fatty acids than the wetland sediments collected at the Malebo Pool with concentrations ranging from 3.3 to 6.0 mg g^{-1} OC (Supplementary Table S4). Their fatty acid composition closely resembled that in the river sediments (Fig. 3). SAFA were the most abundant fatty acids (60.7% to 84.5%) and were dominated by $C_{16:0}$ (13.9% to 27.4%) and LCFA (13.9% in the surface layer at site E to 40.9% in the middle layer at site B) with a strong predominance of $C_{24:0}$ (5.2% to 26.8% of all fatty acids). BAFA were present in all sediment samples (11.7% to 25.6%) with a tendency to be higher in the surface horizons. 3-OH-C_{14} and iso$C_{15:0}$ were the most abundant bacterial fatty acids and were more abundant in the surface sediments. MUFA ranged from 1.2% at the abandoned site E (surface layer) to 13.7% in the channel at site C (mid layer). They were dominated by $C_{16:1\omega7}$, $C_{18:1\omega9cis}$ and $C_{18:1\omega7}$, while $C_{20:1\omega9}$ was present in very small amounts (< 0.4%). A trend to lower MUFA contributions in the surface layers was observed in all the cores except for the one collected in the channel at site A.

PUFA contributions to the sediments were consistently low. However, in the surface sediments collected at the entry of the terminal lobe complex (the channel at site A), the PUFA contribution reached 2.7%, reflected by a higher degree of unsaturation (UI = 23.2, Supplementary Table S4) than in other samples. $C_{20:5\omega3}$ and $C_{22:6\omega3}$ were the predominant PUFA in these surface sediments, whereas $C_{18:2\omega6cis}$ was present in smaller amounts. The CPI varied between 8.4 and 17.5 with lower values at site E, and a trend for higher values with increasing depth. The $ACL_{16–30}$ varied between 19.1 and 22.2.

Fig. 4 shows the downcore distribution of the fatty acids in sediments from the present-day

depocenter (the channel at site C) and the abandoned lobe (site E). LCFA made a substantial contribution to the fatty acid pool at both sites. The contribution of LCFA increased from 14% to 40% with sediment depth in the abandoned lobe (site E), while it accounted for an

average of 25% in the channel at site C with higher contributions in deeper layers (> 16 cm in depth). The contribution of BAFA in the channel at site C remained relatively constant throughout the core (~20%), whereas it decreased by half (from 25%% to 12%) in sediments sampled at site E. At both sites, the contribution of MUFA was remarkably lower in the surface sediment than in the deeper layers with a transition that corresponded to the limit of the oxygen penetration depth (1.47 cm at site C and 6.65 cm at site E; Pozzato et al., 2017). Only trace amounts of PUFA were found at site E, while their contribution reached 4% at site C.

$\delta^{13}C$ values of bulk OM was fairly constant in the channel at site C (~ –26.9‰), whereas terrestrial phytoclasts varied from 25 to 88%. In contrast, $\delta^{13}C$ values of bulk OM decreased progressively with increasing depth at site E (from –23.1‰ to –26.9‰), while terrestrial phytoclasts increased (7% to 84%).

3.5. Clustering and relationships with contextual geochemical and sedimentological parameters

The results of the cluster analysis based on fatty acid composition are shown in Fig. 5. The 42 samples corresponding to seven sites and several sediment horizons (4 to 11 depending of the site) were clustered into four clusters (Fig. 5A). The seven first cm of the core collected at site E formed a single cluster (cluster 4), whereas deeper sediments from this core were grouped with most of the surface sediments from the cores collected in the active lobe (cluster 1). The interval 1–16 cm of the core collected in the channel at site C formed another cluster (cluster 2). The last cluster grouped the deeper layers (16–19 cm and 19–22 cm), the

intermediary layer (5–7 cm) and most surface samples (0–0.5 cm and 0.5–1 cm) from site A (cluster 3). These 4 clusters displayed distinct fatty acid profiles (Fig. 5B).

As sediments from site F accounted for most of the dissimilarity within the dataset, this

site was omitted in the following analyses. The remaining sediment samples were clustered in three clusters with the same partition as observed with the whole dataset (see Supplementary material for HCA results on sediments from the active lobe). The non-metric multidimensional scaling (nMDS) ordination analysis shows the relationships between sediment samples, fatty acid biomarkers and sediment properties defined by grain size, OC content and several proxies of OM origin and quality (Fig. 6). Almost all environmental variables had low p values (< 0.05), indicating highly significant fitted vectors with the exception of sand, OI and $\delta^{15}N$. The highest goodness-of-fit statistics were observed with UI ($r^2 = 0.89$), followed by CPI ($r^2 = 0.78$), ACL ($r^2 = 0.63$), $\delta^{13}C$ ($r^2 = 0.59$) and then DI ($r^2 = 0.47$) (Table 4).

4. Discussion

4.1. Sources of fatty acids in the terminal lobe complex

Fluxes of fatty acids from the surficial ocean to the abyssal plains are usually limited due to the efficient and rapid degradation of these labile components during transit through the water column (Wakeham et al., 1997a). Hence, most deep-sea sediments are characterised by low fatty acid contents and benthic communities are food-limited (Wakeham et al., 1997b; Svetashev, 2022). Fatty acid concentrations in sediments from the Congo deep-sea fan are much higher (between 3.8 and 5.4 mg g^{-1} OC) than the standard background values measured in abyssal plains in the Atlantic Ocean (between 0.02 to 1.04 mg g^{-1} OC; Van Vleet and Quinn, 1979; Santos et al., 1994). These values are high, even in comparison with coastal sediments unaffected by turbidity currents north of the mouth of the Congo River where fatty

acid yields do not exceed 0.96 mg g^{-1} OC (Schefuß et al., 2001). Thus, while deep-sea communities usually only benefit from pulse inputs of labile OM deriving from seasonal and rare planktonic blooms, turbidity flows feed the terminal lobe complex area with a more

persistent (one turbidite every 6–17 years; Dennielou et al., 2017) source of labile components such as functionalised lipids and amino acids (this study and Pruski et al., 2017).

4.1.1. Tracing inputs from the Congo River using glycerol dialkyl glycerol tetraethers and fatty acid biomarkers

The suspended OM delivered by the Congo River is mainly composed of soil-derived mineral associated OM and to a lesser extent of well-preserved plant detritus (Spencer et al., 2012). Knowing that: (1) fine soil particulate OM (< 63 μm) accounts for more than 80% of the total particulate load of the Congo River at Kinshasa (Spencer et al., 2012), and that (2) most of this material is rapidly channelled by turbidity currents to the recent lobe complex (Savoye et al., 2009; Babonneau et al., 2010), soil-derived OM is expected to be a major source of OM in the lobe complex. Using carbon isotopic values in a two-source mixing model, Stetten et al. (2015) previously estimated that the relative proportion of terrestrial OM ranges from 70% to 80% in sediments from the active lobe complex.

Two proxies of terrestrial OM were used in the present study: (1) the branched vs isoprenoid tetraether (BIT) index whose use is based on the initial assumption that branched GDGTs are mainly produced by bacteria in soils, while crenarchaeol is specific for non-extremophilic, aquatic Thaumarchaeota (Hopmans et al., 2004), and (2) LCFA deriving from the epicuticular waxes of higher plants (Eglinton and Hamilton, 1967).

The BIT index was originally introduced as a proxy for the fluvial export of terrestrial OM (Hopmans et al., 2004), but was later shown to trace specifically soil OM (Huguet et al., 2007). BIT index values in suspended particulate matter from the Congo River are close to the

hypothetical terrestrial end-member value of 1 (mean value: 0.98, Weijers, 2017), and decrease in the surface sediments with increasing distance to the estuary, reflecting the fluvial transport of soil OM (Hanmens et al., 2004). It should be noted that over the past decades, the

in situ production of branched GDGTs in marine sediments from different settings has been confirmed, which complicates somewhat the interpretation of GDGT-based proxies (Sinninghe-Damsté, 2016). Branched GDGTs were indeed found in distal marine surface sediments from the Atlantic Ocean, albeit in low amount, and BIT index values were close to the marine end-member value of 0 showing that marine production of branched GDGTs had a limited influence on the BIT index (0.01–0.07; Weijers et al., 2014). Here, BIT values were high (> 0.75, Table 3) in the active lobe area, confirming that soil OM is efficiently exported through the Congo submarine canyon and represents the main source of OM. The significant negative correlation between $\delta^{13}C_{org}$ and the BIT index (Spearman rank correlation, $\rho = -0.69$, p-value < 0.05) further confirms that the BIT index is a good proxy to trace soil inputs in the channel-levee system of the Congo River deep-sea fan, as previously observed in this region (Weijers et al., 2009).

Even though the GDGT results indicate that OM in the actual lobe complex predominantly comes from soil erosion within the Congo watershed, coarse particles deriving from recent vegetation inputs are also exported by the river and represent an additional source of OM (Spencer et al., 2012). Schnyder et al. (2017) highlighted the outstanding good preservation of terrestrial phytoclasts, cuticle particles and wood fragments, which often dominate palynofacies assemblages. Likewise, plant macro-detritus were often observed in our samples (Stetten, personal observation). Hemingway et al. (2016) showed that lipid biomarkers make it possible to get a better picture of the nature of the OM exported by the Congo River and that different classes of lipids reflect different source signals in the watershed, such as BIT index for soil OM, and plant wax lipids for terrestrial plant inputs. Functionalised lipids

(LCFA and alcohols) from plant waxes derive predominantly from a recently reworked local source, whereas *n*-alkanes include a broader watershed signal and have undergone more intense diagenesis (Hemingway et al., 2016). As such, the latter are found in relatively low

amounts in the material exported by the river and subsequently in sediment records from the Congo submarine canyon (e.g., alkane concentrations are 1–2 orders of magnitude lower than those of fatty acids or alcohols; Treignier et al., 2006; Hemingway et al., 2016; Méjanelle et al., 2017).

In the Black Sea, LCFA have been successfully used to trace the dilution of the material delivered by the Danube River with autochthonous OM (Saliot et al., 2002). Sediments from the Malebo Pool consist in a mixture of mineral particles and plant debris, and consequently contain high proportions of LCFA (16.4–28.9% of all fatty acids, Fig. 2). For comparison, the contribution of these higher plant biomarkers is 16% in the Amazon River floodplain (Mortillaro et al., 2011). Their concentration in sediments from the active lobe was high (0.6 to 2.5 mg g^{-1} OC), but consistent with values for the suspended sediments collected in the Congo River (0.97 ± 0.34 mg g^{-1} OC, recalculated from Hemingway et al., 2016).

LCFA are thus exported along with the sediments down to the Congo deep-sea fan where they accumulate in concentrations that are high even when compared to continental margins. This reflects the efficient export and burial of the OM derived from terrestrial plants in the Congo watershed. Nevertheless, LCFA were heterogeneously distributed even across a given core (e.g., Fig. 4a) and did not behave like most bulk geochemical proxies in the study area (Stetten et al., 2015).

In the Rhône pro-delta (France) and in Englebright Lake (California), higher contributions of LCFA were found in sediment layers that recorded flood events and were attributed to higher inputs of macro-detritus (Pondell and Canuel, 2020; Pruski et al., 2021). In good agreement with the hypothesis that the relative abundance of LCFA varies with the proportion

of plant detritus, palynofacies observations confirm that higher plant remains are heterogeneously distributed in the lobe sediments (Schnyder et al., 2017).

Due to their ubiquitous synthesis by different groups of organisms, the contribution of the

other subgroups of fatty acids (SCFA, BAFA, MUFA) are not indicative of OM provenance, but their isotopic values may provide some clues. Generally, lipids such as fatty acids are depleted in ^{13}C relative to total OM (DeNiro and Epstein, 1977). Assuming a $\delta^{13}C_{org}$ value of ~27.5‰ for C_3 land plants (Hedges et al., 1986; Meyers, 1997) and a depletion of 4‰ for fatty acids relative to bulk OC (Wang et al., 1998; Wang and Druffel, 2001), $\delta^{13}C$ values of around –31.5‰ are expected for fatty acids deriving from C_3 plants, whereas inputs from C_4 plants would lead to much higher values (around –18‰; O'Leary, 1988). The light isotopic signature of the saturated fatty acids in the lobe sediments confirms a predominantly terrestrial origin for these compounds ($\delta^{13}C$ $C_{14\text{-}24}$ = –30.8 ± 2.1‰, Supplementary Table S5). These results closely match the range of $\delta^{13}C$ values reported for fatty acids in the suspended particulate matter from the Congo River (–30.9 ± 1.9‰) and are consistent with a strong contribution of OM deriving from C_3 plants, with a negligible influence of C_4 plants (Hemingway et al., 2016). $\delta^{13}C$ values of BAFA and MUFA were less depleted (–29.5 ± 2.7‰ for BAFA and –28.6 ± 2.3‰ for MUFA) than SAFA, but fall within the range of values expected for terrestrial OM (Table 1).

4.1.2. Can we identify marine OM inputs in the terminal lobe complex?

The Congo deep-sea fan is located ~ 5 km below a productive oceanic region characterised by a shallow thermocline, an oceanic upwelling and a river plume, which supply nutrients (Berger, 1989; Schneider et al., 1994). Schefuß et al. (2004) recorded the highest contributions of biomarkers deriving from marine sources in sediments collected about 150–200 km offshore the Congo River mouth. Two PUFA, the dinoflagellate biomarker $C_{22:6\omega3}$ and

the diatom biomarker $C_{20:5\omega3}$, were found in the surface sediments at the entry of the recent lobe complex (67 and 97 µg g^{-1} OC in the channel and levee at site A) despite the depth of

amounts, is unexpected considering that most marine OM that reaches this region is considered to be heavily degraded (Treignier et al., 2006; Stetten et al., 2015). These results demonstrate that biomarkers deriving from fresh phytoplankton can reach the recent lobe complex. Taking into account the rapid degradation of the POM produced in the euphotic layer during settling (Lee et al., 2004), it seems unlikely that the overlying pelagic production could explain the occurrence of phytoplankton PUFA at the entry of the recent lobe complex (site A).

A plausible scenario is that marine POM deposited in the active channel upstream has been caught by turbidity currents and rapidly delivered to the recent lobe complex. A closer look at the fatty acid composition provides further arguments supporting this hypothesis (Supplementary Table S4). $C_{18:1\omega7}$ and $C_{16:1\omega7}$, which are found in many phytoplankton groups including diatoms and dinoflagellates (Volkman et al., 1989; Mansour et al., 1999), were more abundant in sediments collected along the active channel than at site E and their contributions were significantly correlated with the PUFA content in the sediments (Spearman rank correlation, $\rho = 0.81$ and 0.92 for $C_{16:1\omega7}$ and $C_{18:1\omega7}$, p-value < 0.01). Moreover, $C_{16:1\omega7}$ in the surface sediments at site F had a $\delta^{13}C$ signature (–21.3‰, Supplementary Table S5) consistent with an algal origin (Canuel et al., 1997). This observation, however, does not hold when considering the isotopic value of $C_{18:1\omega7}$ and $C_{16:1\omega7}$ in the other samples, whose $\delta^{13}C$ values ranged between –33‰ and –26‰ (Supplementary Table S5). These lower values point to a terrestrial origin, while the less negative values rather suggest a mixture of marine and terrestrial OM (Shi et al., 2001). Since these MUFA are also found in bacteria (Parrish, 2013), their presence in the sediments could also at least partly account for the heterotrophic bacteria

that break down terrestrial and marine OM (Teece et al., 1999; Wang et al., 2008), and their isotopic values would in this case reflect the source of decomposed OM.

Despite the wide array of lipid biomarkers analysed (sterols, alkenones, and short-chain *n*-alkanes in Méjanelle et al. (2017) and fatty acids in the present study), no specific markers of marine primary production were found in appreciable amounts in the lobe sediments, likely due to the degradation of these labile molecules in the water column and the strong dilution of any signal by the turbidity inputs. Overall, fatty acid patterns suggest that fluxes of marine POM are rather limited and that their composition is extensively modified before settling on the seafloor. In good agreement with this: (1) the bulk $\delta^{13}C_{org}$ signature (~ –26.5‰), Rock-Eval pyrolysis analysis and palynofacies observations revealed that marine OM represents at most 30% in these sediments, is highly degraded, and is present as amorphous material (Stetten et al., 2015; Baudin et al., 2017b; Schnyder et al., 2017).

This marine fraction is also highlighted by the BIT index, which takes into account in its calculation crenarchaeol as the marine end-member (Hopmans et al., 2004). Since crenarchaeol is a membrane lipid produced by archaea, the link between this marker and phytoplankton production is unclear, but the coupling between the concentrations of chlorines (indicative of phytoplankton production) and crenarchaeol has been observed in sedimentary archives (Fietz et al., 2011). Crenarchaeol abundance was relatively constant in the lobe sediments (1.1 ± 0.3 µg g^{-1} dw), but was not correlated to PUFA concentrations, probably because the ether bonds of the archaeal marker ensure better preservation.

4.1.3. Transformation of the source signal during transport

The challenge to assess sink to source transformations lies in the difficulty to constrain the original source signatures and the limited knowledge on the many factors that control the chemical composition of the exported OM. The Malebo Pool is recognised as a good

sampling location for Congo suspended solids because no major tributary enters the river between Kinshasa and the head of the estuary (~350 km downstream), and the POM composition remains fairly constant from this point to the mouth of the river (Spencer et al.

2012). Soil-OM from the Congo watershed is deposited in the Malebo Pool wetlands and later exported to the Atlantic Ocean with some local production (Talbot et al., 2014; Spencer-Jones et al., 2015). Sediments from the Malebo Pool displayed OC-normalised concentrations in fatty acids similar to that of river-suspended POM (Hemingway et al., 2016) confirming that they are representative of the terrestrial OM exported by the Congo River. The higher LCFA abundance in the Malebo Pool wetlands relative to the river POM is consistent with the integration of the local C_3-vegetation signal. Low contribution of unsaturated homologues in permanently submerged and recently exposed sediments are indicative of degraded OM.

Using radiocarbon measurements, Hemingway et al. (2017) have demonstrated that deposits in the cuvette Congolaise swamp forest are significantly older than those sourced from other ecosystems and that this material is exported by the Congo River. Although the extent of OM degradation in the Malebo Pool is certainly less than in the cuvette Congolaise, these observations combine with the different proxies of OM alteration used here and in previous studies are strong evidences for OM pre-aging within the watershed prior export to the Congo shelf and deep-sea fan (UI, amino acid based indices DI and RI, Rock-Eval OI and HI, palynofacies; Baudin et al., 2017b; Pruski et al., 2017; Schnyder et al., 2017).

Sediments in the active lobe area have a fatty acid composition that closely matches that of the permanently submerged and recently exposed sediments from the Malebo Pool in terms of proportion of major components highlighting the remarkably good preservation of the terrestrial source signal in spite of the distance covered. Fatty acids are considered as relatively labile lipid biomarkers and undergo rapid degradation in the ocean. However, the degradation rate of each fatty acid depends on many factors including its chemical structure,

the phase with which it is associated, and the exposure time to O_2 (Bianchi and Canuel, 2011). If the fatty acids exported by the Congo River undergo extensive degradation during their transport, one would expect a marked decrease of the OC-normalised concentrations from the source to the terminal depocenter (site C). This was not the case, either suggesting that fatty acids are degraded at the same rate as total OC or that OM remineralisation is low.

The OC content in the sediments shows no notable evolution from the estuary to the distal reach of the Congo deep-sea fan: 2.9% in the estuary (Schefuß et al., 2004), 3.6% at a water depth of 962 m (Weijers et al. 2009), 2.5% to 4.5% at a water depth of 2000 m (Mariotti et al., 1991), 3.0±0.6 and 3.1±0.6 at water depths of 4000 m and 4150 m (Baudin et al., 2010), and 3.2±0.6 in the present-day terminal lobe complex (~5000 m, this study). This observation and the fact that sediments from the lobe complex and the Malebo Pool have similar fatty acid profiles and comparable values of microbial degradation indices (UI, CPI and $ACL_{16–30}$) support the hypothesis that terrestrial OM delivered by the Congo River undergoes limited reprocessing during the 1135 km transit to the terminal lobe area.

This lack of apparent reactivity may be attributed to the nature of the POM exported by the river, which is mostly associated to soils (Spencer et al., 2012; Hemingway et al., 2017). Fatty acids deriving from both plant materials and microorganisms are vulnerable to decomposition by microbial decomposers, but interactions with mineral surfaces and occlusion in soil aggregates may stabilize and protect them from degradation (Salmon et al., 2000; Lützow et al., 2006; Wakeham et al., 2009). Leaf plant waxes were shown to have a particularly high affinity for the inorganic matrix, higher than that of other plant markers such as lignin phenols (Feng et al., 2013). The interaction of leaf fatty acids with organo-mineral aggregates may limit their degradation and allow the export of pre-aged, but yet reactive, pools of OC.

The dynamic of sediment transfer in the Congo turbiditic system is another factor which may contribute to the preservation of fatty acids. Sediment transfer is non-linear with phases

of deposition and erosion all along the canyon and the channel, but OM burial is always prevalent (Talling et al., 2022). The speed at which turbidity currents export the terrigenous particles to the terminal lobe area limits the exposure time to O_2 and allows the preservation of recent plant remains in the sediments with limited alteration of their structural lipid content (Schnyder et al., 2017, Talling et al., 2022).

4.2. Processes affecting fatty acid preservation

Fatty acid profiles were used to explore post-depositional processes involved with the preservation of these compounds in recent turbidites. To explore this aim, groups of samples with similar fatty acid composition were determined (Fig. 5) and related to the geochemical proxies determined concurrently from the same cores (Fig. 6). The sediment samples were partitioned into four distinct clusters, each characterised by different biomarker composition, geochemical properties and grain size distribution, providing clues on the factors affecting OM distribution and preservation in the distal reach of the Congo turbiditic system.

4.2.1. Post-depositional oxic degradation

When a turbidite settles in the deep ocean, oxygen from the overlying surface water diffuses in the deposit until equilibrium is reached. This controls the evolution of the redox conditions and the extent of oxic degradation (Wilson et al., 1985). Consequently, turbidites have been considered as an interesting in situ model for the study of long-term oxic degradation (de Lange, 1998; Hoefs et al., 2002; Huguet et al., 2008), but this approach has not been applied to recent turbidite deposits, such as those in the Congo terminal lobe complex where oxygen diffusion into the surface of the turbidite is restricted to the first centimetre (Pozzato et al., 2017).

The nMDS ordination of the samples from the active lobe area confirms that surface sediments (layers 0–0.5 cm and 0.5–1 cm in cluster 1) had a fatty acid composition distinct from that of the deeper layers (Fig. 6). Higher PARA contributions in the surface sediments

are consistent with an enhanced bacterial degradation near the benthic boundary layer where more electron acceptors are present, especially O_2 (Emerson and Hedges, 2006), whereas lower contributions of MUFA and PUFA show the preferential degradation of unsaturated compounds, which are more labile. These sediments were also characterised by lower OC contents, consistent with increased degradation in oxic conditions, as well as lower values of our amino acid and fatty acid-based proxies of OM quality (UI and DI) indicative of a more advanced alteration of the OM.

$\delta^{13}C$ values of bulk OC were also higher in the surface sediments which was also observed for many fatty acids (Supplementary Table S5). Diagenesis might explain this positive isotopic shift and could be due to the selective degradation of ^{13}C-depleted components, such as lipids (Sun et al., 2004; Pan et al., 2014). Sun et al. (2004) further postulated that ^{13}C enrichment of fatty acids during decomposition could be attributed to the dissimilar distribution of ^{13}C between carbon sites and the dominant decarboxylation pathway, which removes the isotopically lighter carboxyl group, leading to higher $\delta^{13}C$ of the residual fatty acids. Surface sediments collected at the entry of the terminal lobe complex (site A) were not clustered with the other upper layers due to a higher contribution of PUFA. Nevertheless, there are also evidences of oxic degradation at this site with a decrease of the OC content by about one fourth between the non-oxidised and the oxidised layers and lower values of the degradation index (DI) at the surface.

The particulate OM resuspended during turbidity events is strongly remineralised before settling on the seafloor (Vangriesheim et al., 2009). The efficient degradation of the material resuspended by turbidity currents and deposited in the fluffy layer was previously

demonstrated in the Congo canyon-levee system using alcohol biomarkers (Treignier et al., 2006). A decrease of 62% of the total *n*-alcohols was observed between the material in suspension collected during the turbidite event and 9 months later in the surface sediment. To assess the extent of post-depositional degradation on fatty acid concentration in the terminal lobe complex, we calculated preservation factors in a similar way to that described by Hoefs et al. (2002) (Table 5). The extent of degradation observed here for fatty acid biomarkers was lower than in the study of Treignier et al. (2006), but only accounts for the oxic degradation taking place in the first upper oxic layer after deposition of the turbidite, as no information on the composition of the material in suspension during the last turbidite event was available. SCFA decreased by 3–33% between the non-oxidised (3–5 cm) and the oxidised (0–0.5 cm) layers with strong differences between individual fatty acids. Preservation factors for $C_{14:0}$ were constantly above 100%, suggesting post-depositional production of this compound in the oxic layer. MUFA and PUFA were more extensively degraded than SCFA (> 40%) apart from in the channel at site A, which received additional inputs of phytoplankton biomarkers.

The level of alteration of the different fatty acid subgroups followed their known level of resistance to oxidation, with higher plant biomarkers being the less prone to degradation (Wakeham et al., 1997a). Preservation factors for most bacterial biomarkers are higher than 100%, suggesting in situ production of these compounds by aerobic heterotrophs. By contrast, preservation factors above 100% for certain LCFA biomarkers might be indicative of the heterogeneous distribution of plant detritus (see Section 4.2.2).

Oxic degradation appears as the principal process affecting fatty acid preservation in the terminal lobe area but is strictly restricted to the uppermost sediment layer (~ first cm), consistent with the depth of oxygen penetration, which never exceeded 1.8 cm (Pozzato et al., 2017). In relict turbidites from the Madeira abyssal plain, dissolved oxygen has been diffusing into the sediments for thousands of years, which explains the presence of a marked oxygen

front separating OM-depleted surface sediments and well-preserved OM in deep sediments (Cowie et al., 1995; Prahl et al., 1997; de Lange, 1998). In these deposits, 80% of the organic carbon and 50% of the nitrogen originally present in the sediment have been degraded under oxic conditions (de Lange, 1998). By contrast, in the recent lobe complex, even if mineralisation rates are exceptional for this depth (Rabouille et al., 2009), OM loss remains limited to the surface sediments and burial clearly outweighs remineralisation processes: ~ 12% to 35% of the OC initially deposited in the upper oxic layer is degraded.

4.2.2. Deposition dynamics and lateral sorting

A remarkable feature of the Congo turbidite system is the homogenous composition and distribution of the OM in the channel-levee area and in the terminal lobe complex at different scales, from the single turbiditic event to the entire lobe area (Baudin et al., 2010, 2017b; Stetten et al., 2015). This apparent homogeneity may be explained by the predominant export of fine-grained particles by the Congo River, which limits hydrodynamic sorting by the turbidity currents as well as by post-depositional sediment reworking (Stetten et al., 2015; Baudin et al., 2017b). Multivariate analyses of the fatty acid profiles nonetheless revealed site differences in the distribution of terrestrial biomarkers, which were related to subtle changes in sediment grain size: the layers 1 cm to 16 cm of the core collected in the channel of site C were grouped in cluster 2, while the 16–22 cm layers were grouped in cluster 3 with the 5–7 and 19–22 cm layers of the other sites. High contributions of terrestrial plant biomarkers (LCFA) and high CPI values along with higher C/N ratios and a slightly coarser granulometry in cluster 3 are indicative of the preservation of plant detritus. In contrast, lower contributions of LCFA in conjunction with lower ACL values and a higher proportion of clay in cluster 2 point to higher inputs of soil-derived OM in the channel at site C.

The density/buoyancy sorting of particles that occurs along the active channel-levee system (Schnyder et al., 2017) may explain the lower proportion of plant debris observed in the main depositional area (channel at site C). Site C, located at the end of the feeding

channel, is the terminal depocenter of materials transported by the Congo canyon system (Babonneau et al., 2010; Dennielou et al., 2017). Thus, this site mostly accumulates fine particles from soils, as plant debris form low density aggregates that can be sorted upstream (Remusat et al., 2012; Cotrufo et al., 2015). High UI, DI and OC content associated with these sediments further show the limited diagenetic changes occurring in these anaerobic sediments and underline the good preservation of the OM in the terminal depocenter.

A mechanism often proposed to explain OM preservation is its strong association with the mineral matrix (Huguet et al., 2008). As stated earlier, OM is mainly associated with fine silty-clay minerals in the lobe sediments (Stetten et al., 2015). The labile compounds can be adsorbed on mesopores present on the surface of these small particles (Mayer, 1994), which protects the intrinsically labile OM from microbial enzymes (Wakeham and Canuel, 2006). The increased contribution of soils and the exceptionally high accumulation rates (up to 12 cm y^{-1} at site C; Stetten et al., 2015; Rabouille et al., 2017) very likely account for the higher preservation potential in the terminal depocenter. Besides, physical disturbance is certainly lower due to the loss of confinement, which limits sediment re-exposure to oxygen.

4.2.3. Past and actual influence of turbidity currents on the abandoned lobe

The terminal lobe complex of the Congo turbidite system has been formed by the successive progradation of the turbidite deposits. Site E corresponds to an older lobe, which got disconnected after the bifurcation to the south of the active channel between 4000 to 6000 years ago (Picot et al., 2016). Despite this, sediments in the active and abandoned lobes still share some common features. A high OC content compared to the surrounding abyssal plains

of the equatorial Atlantic Ocean (Baudin et al., 2017a) and the presence of LCFA along with a BIT value ranging between 0.48 and 0.76 show the past and actual influence of the Congo channel-levee system on the abandoned lobe. Fig. 4b illustrates the changes in the proportion

of land-derived OM proxies (e.g., proportions of LCFA and terrestrial phytoclasts), reflecting the progressive shift from terrestrial inputs supplied by ancient turbidite events to the present-day hemipelagic sedimentation. The first 7 cm of this core formed a distinct cluster characterised by the absence of PUFA, lower MUFA content and higher contributions of SCFA (Fig. 5, cluster 4). These sediments are of marine origin as evidenced by their $\delta^{13}C_{org}$ signature, which was significantly higher than the mean $\delta^{13}C_{org}$ of all the samples (Stetten et al., 2015).

The hypothesis of the hemipelagic origin of OM in the topmost layers of site E is strengthened by the higher $\delta^{13}C$ values of the fatty acids (Supplementary Table S5). This hemipelagic ooze consists in the sedimentation of marine particles with the admixture of terrigenous material originating from the dispersion and settling of the upper turbid plume of the turbidites deposited ~40 km to the south and/or from the pelagic snow. These inputs explain the presence of terrestrial biomarkers in the surface sediments of the abandoned site (this study and Méjanelle et al., 2017) as well as the occurrence of terrestrial amorphous OM and plant debris (Stetten et al., 2015; Schnyder et al., 2017). Higher OI and lower DI are furthermore associated with these layers, indicative of a strongly oxidised OM (Table 1). This is consistent with the high penetration depth of oxygen (~6 cm on Fig. 4b, Pozzato et al., 2017) and the low sedimentation rate at this site (Rabouille et al., 2017), which provide favourable conditions for the intensive oxidation of the hemipelagic deposit.

Below a depth of 7 cm, sediments from the abandoned site displayed a fatty acid composition similar to that of the surface sediments from the active lobe (cluster 1, Fig. 5), suggesting that they correspond to ancient turbidite deposits. The clustering of these

sediments with the oxic layers from the active lobe shows that the OM has been subjected to some degradation, but the persistence of fatty acids in these ancient turbidites over millennia is nonetheless remarkable. As already mentioned, LCFA are associated with soil aggregates

mineral particles or plant remains consisting of relatively recalcitrant substances such as lignin or cellulose and may thus be protected from microbial degradation (Wakeham and Canuel, 2006). Such a good preservation of the fatty acid record suggests the progressive burial of the older turbidite deposit under the predominantly hemipelagic sedimentation without any significant reworking or redistribution of the sediments on the abyssal plain over the past few millennia.

5. Conclusions

Sediment cores from the terminal lobe complex of the Congo deep-sea fan were investigated to assess the potential of fatty acids as biomarkers of OM origin and processes affecting the composition of the terrestrial material transported by turbidity currents during transit in the channel-levee system and after deposition in the distal depositional area. Fig. 7 summarises the major outcomes from this study. The close similarity of the molecular composition of sediments from the active lobe with that of samples collected on land at the Malebo Pool suggests that: (1) POM delivered by the Congo River is primarily composed of soil-OM deriving from C_3 plants, (2) OM is subjected to limited recycling during transit, and (3) mixing of riverine inputs with material from the surrounding Angola margin is low. Yet, the unexpected occurrence of undegraded phytoplankton biomarkers at the entrance of the terminal lobe highlights the fact that pelagic inputs deposited upstream in the active channel may be rapidly exported by turbidity currents. Long chain fatty acids were used to trace inputs from the Congo River at different time scales and their good preservation in the ancient turbidites suggests a conservative behaviour. This study revealed the different mobilisation

pathways for the OM associated with fine soil-derived particles and the coarser plant detritus, likely related with the density/buoyancy sorting taking place in the turbidity currents and the resulting selective delivery. Quantitative estimates of both the soil and plant terrestrial inputs in the Congo lobe complex are still lacking, but the combination of fatty acid and glycerol dialkyl glycerol tetraether biomarkers offers promising perspectives to better deconvolute the soil-derived OM and the plant debris signals.

Acknowledgements

We are indebted to Ifremer/Genavir, captain (G. Ferrand), chief scientist (C. Rabouille), and the crew for the sampling campaign Congolobe onboard the R/V *Pourquoi Pas?* We acknowledge S. Bourgeois for processing the samples during the Congolobe campaign as well as B. Bombled and P. Noel in charge of multicore sampling during the cruise. We also thank R. Spencer and H. Talbot for providing samples from the Congo River. We are grateful to M.Y. Sun who initiated the collaboration with the Center for Applied Isotope Studies (University of Georgia), and R. Culp and H. Pan who performed the compound specific isotopic analyses. We appreciate the assistance of J. Caparros and O. Crispi who kindly performed elemental analyses on the river samples, and A. Lethiers for participating in the drawings. Finally, we acknowledge B. Dennielou for fruitful comments on this paper. This work was supported by the ANR grant Congolobe led by C. Rabouille (ANR Blanc SIMI5-6, n°11 BS56 030). The study also benefited from financial support from the Institute of Ecology and Environment (INEE CNRS and University Paris VI) to UMR8222 LECOB. E. Stetten was supported by a doctoral fellowship from the French Ministry of Research and Education. We are grateful to the Co-Editor in Chief J. Volkman, Associate Editor I. S. Castañeda, and reviewers D. He and V. Galy for their thoughtful comments and constructive suggestions, which helped to further improve this manuscript.

Associate Editor–**Isla Castañeda**

References

Angst, G., John, S., Mueller, C.W., Kögel-Knabner, I., Rethemeyer, J., 2016. Tracing the sources and spatial distribution of organic carbon in subsoils using a multi-biomarker approach. Scientific Reports 6, 29478.

Azpiroz-Zabala, M., Cartigny, M.J.B., Talling, P.J., Parsons, D.R., Sumner, E.J., Clare, M.A., Simmons, S.M., Cooper, C., Pope, E.L., 2017. Newly recognized turbidity current structure can explain prolonged flushing of submarine canyons. Science Advances doi:10.1126/sciadv.1700200

Babonneau, N., Savoye, B., Cremer, M., Bez, M., 2010. Sedimentary architecture in meanders of a submarine channel: detailed study of the present Congo turbidite channel (Zaiango Project). Journal of Sedimentary Research 80, 852–866.

Badewien, T., Vogts, A., Rullkötter, J., 2015. *n*-Alkane distribution and carbon stable isotope composition in leaf waxes of C_3 and C_4 plants from Angola. Organic Geochemistry 89–90, 71–79.

Bao, R., Zhao, M., McNichol, A., Wu, Y., Guo, X., Haghipour, N., Eglinton, T.I., 2019. On the origin of aged sedimentary organic matter along a river-shelf-deep ocean transect. Journal of Geophysical Research: Biogeosciences 124, 2582–2594.

Baudin, F., Disnar, J.R., Martinez, P., Dennielou, B., 2010. Distribution of the organic matter in the channel-levees systems of the Congo mud-rich deep-sea fan (West Africa). Implication for deep offshore petroleum source rocks and global carbon cycle. Marine and Petroleum Geology 27, 995–1010.

Baudin, F., Disnar, J.-R., Aboussou, A., Savignac, F., 2015. Guidelines for Rock-Eval analysis of recent marine sediments. Organic Geochemistry 86, 71–80.

Baudin, F., Martinez, P., Dennielou, B., Charlier, K., Marsset, T., Droz, L., Rabouille, C., 2017a. Organic carbon accumulation in modern sediments of the Angola basin

influenced by the Congo deep-sea fan. Deep Sea Research Part II: Topical Studies in Oceanography 142, 64–74.

Baudin, F., Stetten, E., Schnyder, J., Charlier, K., Martinez, P., Dennielou, B., Droz, L.,

2017b. Origin and distribution of the organic matter in the distal lobe of the Congo deep-sea fan – A Rock-Eval survey. Deep Sea Research Part II: Topical Studies in Oceanography 142, 75–90.

Baudin, F., Rabouille, C., Dennielou, B., 2020. Routing of terrestrial organic matter from the Congo River to the ultimate sink in the abyss: a mass balance approach. Geologica Belgica doi:10.20341/gb.2020.004

Benner, R., 2004. What happens to terrestrial organic matter in the ocean? Marine Chemistry 92, 307–310.

Berger, W.H., 1989. Global maps of ocean productivity. In: Berger, W.H., Smetacek, V.S., Wefer, G. (Eds.), Productivity of the Ocean: Present and Past. Wiley, Dahlem Konferenzen, pp. 429–455.

Bianchi, T.S., Allison, M.A., Cai, W.-J., 2014. An introduction to the biogeochemistry of river-coastal systems. In: Biogeochemical Dynamics at Major River-Coastal Interfaces: Linkages with Global Change. Cambridge University Press, Cambridge.

Bianchi, T.S., Canuel, E.A., 2011. Chapter 8. Lipids: Fatty acids. In: Chemical Biomarkers in Aquatic Ecosystems. Princeton University Press, USA.

Blair, N.E., Aller, R.C., 2012. The fate of terrestrial organic carbon in the marine environment. Annual Review of Marine Science 4, 401–423.

Bonnel, C., 2005. Mise en place des lobes distaux dans les systèmes turbiditiques actuels : analyse comparée des systèmes du Zaïre, Var, et Rhône (Thèse de doctorat). Bordeaux 1.

Bourgeois, S., Pruski, A.M., Sun, M.-Y., Buscail, R., Lantoine, F., Kerhervé, P., Vétion, G., Rivière, B., Charles, F., 2011. Distribution and lability of land-derived organic matter in the surface sediments of the Rhône prodelta and the adjacent shelf (Mediterranean Sea, France): a multi proxy study. Biogeosciences 8, 3107–3125.

Buckley, D.E., Cranston, R.E., 1988. Early diagenesis in deep sea turbidites: The imprint of paleo-oxidation zones. Geochimica et Cosmochimica Acta 52, 2925–2939.

Budge, S.M., Parrish, C.C., McKenzie, C.H., 2001. Fatty acid composition of phytoplankton, settling particulate matter and sediments at a sheltered bivalve aquaculture site. Marine Chemistry 76, 285–303.

Burdige, D.J., 2005. Burial of terrestrial organic matter in marine sediments: A re-assessment. Global Biogeochemical Cycles 19, 7 pp.

Cadée, G.C., 1984. Particulate and dissolved organic carbon and chlorophyll A in the Zaire river, estuary and plume. Netherlands Journal of Sea Research 17, 426–440.

Canuel, E.A., Freeman, K.H., Wakeham, S.G., 1997. Isotopic compositions of lipid biomarker compounds in estuarine plants and surface sediments. Limnology and Oceanography 42, 1570–1583.

Claustre, H., Poulet, S., Williams, R., Ben-Mlih, F., Martin-Jézéquel, V., Marty, J.C., 1992. Relationship between the qualitative nature of particles and copepod feces in the Irish Sea. Marine Chemistry 40, 231–248.

Coffinet, S., Huguet, A., Williamson, D., Fosse, C., Derenne, S., 2014. Potential of GDGTs as a temperature proxy along an altitudinal transect at Mount Rungwe (Tanzania). Organic Geochemistry 68, 82–89.

Cotrufo, M.F., Soong, J.L., Horton, A.J., Campbell, E.E., Haddix, M.L., Wall, D.H., Parton, W.J., 2015. Formation of soil organic matter via biochemical and physical pathways of litter mass loss. Nature Geoscience 8, 776–779.

Cowie, G.L., Hedges, J.I., Prahl, F.G., de Lange, G.J., 1995. Elemental and major biochemical changes across an oxidation front in a relict turbidite: An oxygen effect. Geochimica et Cosmochimica Acta 59, 33–46.

Coynel, A., Seyler, P., Etcheber, H., Meybeck, M., Orange, D., 2005. Spatial and seasonal dynamics of total suspended sediment and organic carbon species in the Congo River. Global Biogeochemical Cycles 19, doi:10.1029/2004GB002335

Dai, J., Sun, M., Culp, R., Noakes, J., 2009. A laboratory study on biochemical degradation and microbial utilization of organic matter comprising a marine diatom, land grass, and salt marsh plant in estuarine ecosystems. Aquatic Ecology 43, 825–841.

Dauwe, B., Middelburg, J.J., Herman, P.M.J., Heip, C.H.R., 1999. Linking diagenetic alteration of amino acids and bulk organic matter reactivity. Limnology and Oceanography 44, 1809–1814.

de Lange, G., 1998. Oxic vs. anoxic diagenetic alteration of turbiditic sediments in the Madeira abyssal plain, eastern North Atlantic. In: Proceedings of the Ocean Drilling Program; Scientific Results; Gran Canaria and Madeira Abyssal Plain; Covering Leg 157 of the Cruises of the Drilling Vessel JOIDES Resolution, Bridgetown, Barbados, to Las Palmas, Canary Islands, Sites 950-956, 24 July-23 September 1994. Texas A & M University, Ocean Drilling Program, College Station, TX, United States, pp. 573–580.

Delègue, M.-A., Fuhr, M., Schwartz, D., Mariotti, A., Nasi, R., 2001. Recent origin of a large part of the forest cover in the Gabon coastal area based on stable carbon isotope data. Oecologia 129, 106–113.

DeNiro, M.J., Epstein, S., 1977. Mechanism of carbon isotope fractionation associated with lipid synthesis. Science 197, 261–263.

Dennielou, B., Droz, L., Babonneau, N., Jacq, C., Bonnel, C., Picot, M., Le Saout, M., Saout, Y., Bez, M., Savoye, B., Olu, K., Rabouille, C., 2017. Morphology, structure, composition and build-up processes of the active channel-mouth lobe complex of the Congo deep-sea fan with inputs from remotely operated underwater vehicle (ROV) multibeam and video surveys. Deep Sea Research Part II: Topical Studies in Oceanography 142, 25–49.

Dettmer, K., Stevens, A.P., Fagerer, S.R., Kaspar, H., Oefner, P.J., 2012. Amino acid analysis in physiological samples by GC–MS with propyl chloroformate derivatization and iTRAQ–LC–MS/MS. In: Alterman, M.A., Hunziker, P. (Eds.), Amino Acid Analysis, Methods in Molecular Biology. Humana Press, pp. 165–181.

Ding, H., Sun, M.-Y., 2005. Biochemical degradation of algal fatty acids in oxic and anoxic sediment-seawater interface systems: effects of structural association and relative roles of aerobic and anaerobic bacteria. Marine Chemistry 93, 1–19.

Dunstan, G.A., Volkman, J.K., Barrett, S.M., Leroi, J.M., Jeffrey, S.W., 1994. Essential polyunsaturated fatty acids from 14 species of diatom (Bacillariophyceae). Phytochemistry 35, 155–161.

Eglinton, G., Hamilton, R.J., 1967. Leaf epicuticular waxes. Science 156, 1322–1335.

Emerson, S.R., Hedges, J.I., 2006. Benthic fluxes and early diagenesis, in: The Oceans and Marine Geochemistry, Treatise on Geochemistry. Elsevier, Amsterdam, pp. 293–316.

Espitalié, J., Deroo, G., Marquis, F., 1985. La pyrolyse Rock-Eval et ses applications. Deuxième partie. Revue de l'Institut Français du Pétrole 40, 755–784.

Feng, X., Vonk, J.E., Dongen, B.E. van, Gustafsson, Ö., Semiletov, I.P., Dudarev, O.V., Wang, Z., Montluçon, D.B., Wacker, L., Eglinton, T.I., 2013. Differential mobilization of terrestrial carbon pools in Eurasian Arctic river basins. Proceedings of the National Academy of Sciences 110, 14168–14173.

Fietz, S., Martínez-Garcia, A., Rueda, G., Peck, V.L., Huguet, C., Escala, M., Rosell-Melé, A., 2011. Crenarchaea and phytoplankton coupling in sedimentary archives: Common trigger or metabolic dependence? Limnology and Oceanography 56, 1907–1916.

Fischer, G., Miller, P.J., Wefer, G., 1998. Latitudinal δ^{13}Corg variations in sinking matter and sediments from the South Atlantic: effects of anthropogenic CO_2 and implications for paleo-pCO_2 reconstructions. Journal of Marine Systems 17, 471–495.

Hedges, J.I., Clark, W.A., Quay, P.D., Richey, J.E., Devol, A.H., Santos, U. de M., 1986. Compositions and fluxes of particulate organic material in the Amazon River. Limnology and Oceanography 31, 717–738.

Hedges, J.I., Keil, R.G., 1995. Sedimentary organic matter preservation: an assessment and speculative synthesis. Marine Chemistry 49, 81–115.

Hedges, J.I., Keil, R.G., Benner, R., 1997. What happens to terrestrial organic matter in the ocean? Organic Geochemistry 27, 195–212.

Hedges, J.I., Oades, J.M., 1997. Comparative organic geochemistries of soils and marine sediments. Organic Geochemistry 27, 319–361.

Heezen, B.C., Menzies, R.J., Schneider, E.D., Ewing, W.M., Granelli, N.C.L., 1964. Congo submarine Canyon. American Association of Petroleum Geologists Bulletin 48, 1126–1149.

Hemingway, J.D., Schefuß, E., Dinga, B.J., Pryer, H., Galy, V.V., 2016. Multiple plant-wax compounds record differential sources and ecosystem structure in large river catchments. Geochimica et Cosmochimica Acta 184, 20–40.

Hemingway, J., 2017. Understanding terrestrial organic carbon export: a time-series approach. PhD thesis, Joint Program in Chemical Oceanography (Massachusetts Institute of Technology, Department of Earth, Atmospheric, and Planetary Sciences; and the Woods Hole Oceanographic Institution), 190 pages.

Hemingway, J.D., Schefuß, E., Spencer, R.G.M., Dinga, B.J., Eglinton, T.I., McIntyre, C., Galy, V.V., 2017. Hydrologic controls on seasonal and inter-annual variability of Congo River particulate organic matter source and reservoir age. Chemical Geology 466, 454–465.

Hoefs, M.J.L., Rijpstra, W.I.C., Sinninghe Damsté, J.S., 2002. The influence of oxic degradation on the sedimentary biomarker record I: evidence from Madeira Abyssal Plain turbidites. Geochimica et Cosmochimica Acta 66, 2719–2735.

Hopmans, E.C., Weijers, J.W.H., Schefuß, E., Herfort, L., Sinninghe Damsté, J.S., Schouten, S., 2004. A novel proxy for terrestrial organic matter in sediments based on branched and isoprenoid tetraether lipids. Earth and Planetary Science Letters 224, 107–116.

Huguet, C., de Lange, G.J., Gustafsson, Ö., Middelburg, J.J., Sinninghe Damsté, J.S., Schouten, S., 2008. Selective preservation of soil organic matter in oxidized marine sediments (Madeira Abyssal Plain). Geochimica et Cosmochimica Acta 72, 6061–6068.

Huguet, C., Hopmans, E.C., Febo-Ayala, W., Thompson, D.H., Sinninghe Damsté, J.S., Schouten, S., 2006. An improved method to determine the absolute abundance of glycerol dibiphytanyl glycerol tetraether lipids. Organic Geochemistry 37, 1036–1041.

Huguet, C., Smittenberg, W.B., Boer, W., Sinninghe Damsté, S., Schouten, S., 2007. Twentieth century proxy records of temperature and soil organic matter input in the Drammensfjord, southern Norway. Organic Geochemistry 38, 1838–1849.

Lee, C., Wakeham, S., Arnosti, C., 2004. Particulate organic matter in the sea: the composition conundrum. AMBIO: A Journal of the Human Environment 33, 565–575.

Lützow, M.V., Kögel-Knabner, I., Ekschmitt, K., Matzner, E., Guggenberger, G., Marschner, B., Flessa, H., 2006. Stabilization of organic matter in temperate soils: mechanisms

and their relevance under different soil conditions – a review. European Journal of Soil Science 57, 426–445.

Maechler, M., Rousseeuw, P., Struyf, A., Hubert, M., Hornik, K., 2019. cluster: Cluster Analysis Basics and Extensions. R package version 2.1.0. cluster package v2.1.0 [WWW Document]. URL https://www.rdocumentation.org/packages/cluster/versions/2.1.0 (accessed 1.19.21).

Mansour, M.P., Volkman, J.K., Jackson, A.E., Blackburn, S.I., 1999. The fatty acid and sterol composition of five marine dinoflagellates. Journal of Phycology 35, 710–720.

Mayer, L.M., 1994. Surface area control of organic carbon accumulation in continental shelf sediments. Geochimica et Cosmochimica Acta 58, 1271–1284.

Mayer, L.M., Schick, L.L., Hardy, K.R., Wagai, R., McCarthy, J., 2004. Organic matter in small mesopores in sediments and soils. Geochimica et Cosmochimica Acta 68, 3863–3872.

Méjanelle, L., Rivière, B., Pinturier, L., Khripounoff, A., Baudin, F., Dachs, J., 2017. Aliphatic hydrocarbons and triterpenes of the Congo deep-sea fan. Deep Sea Research Part II: Topical Studies in Oceanography 142, 109–124.

Meyers, P.A., 1997. Organic geochemical proxies of paleoceanographic, paleolimnologic, and paleoclimatic processes. Organic Geochemistry 27, 213–250.

Moloney, C.L., Field, J.G., 1991. The size-based dynamics of plankton food webs. I. A simulation model of carbon and nitrogen flows. Journal of Plankton Research 13, 1003–1038.

Mortillaro, J.M., Abril, G., Moreira-Turcq, P., Sobrinho, R.L., Perez, M., Meziane, T., 2011. Fatty acid and stable isotope ($\delta^{13}C$, $\delta^{15}N$) signatures of particulate organic matter in the lower Amazon River: Seasonal contrasts and connectivity between floodplain lakes and the mainstem. Organic Geochemistry 42, 1159–1168.

Oksanen, J., Blanchet, F.G., Friendly, M., Kindt, R., Legendre, P., McGlinn, D., Minchin, P.R., O'Hara, R.B., Simpson, G.L., Solymos, P., Henry, M., Stevens, H., E Szoecs, Wagner, H., 2016. vegan: Community Ecology Package. CRAN: The Comprehensive R Archive Network.

O'Leary, M.H., 1988. Carbon isotopes in photosynthesis. BioScience 38, 328–336.

Pan, H., Culp, R.A., Noakes, J.E., Sun, M.-Y., 2014. Effects of growth stages, respiration, and microbial degradation of phytoplankton on cellular lipids and their compound-specific stable carbon isotopic compositions. Journal of Experimental Marine Biology and Ecology 461, 7–19.

Parrish, C.C., 2013. Lipids in Marine Ecosystems. ISRN Oceanography 2013, e604045.

Picot, M., Droz, L., Marsset, T., Dennielou, B., Bez, M., 2016. Controls on turbidite sedimentation: Insights from a quantitative approach of submarine channel and lobe architecture (Late Quaternary Congo Fan). Marine and Petroleum Geology 72, 423–446.

Picot, M., Marsset, T., Droz, L., Dennielou, B., Baudin, F., Hermoso, M., de Rafelis, M., Sionneau, T., Cremer, M., Laurent, D., Bez, M., 2019. Monsoon control on channel avulsions in the Late Quaternary Congo Fan. Quaternary Science Reviews 204, 149–171.

Pondell, C.R., Canuel, E.A., 2020. Sterol, fatty acid, and lignin biomarkers identify the response of organic matter accumulation in Englebright Lake, California (USA) to climate and human impacts. Organic Geochemistry 142, 103992.

Powers, J.S., Schlesinger, W.H., 2002. Geographic and vertical patterns of stable carbon isotopes in tropical rain forest soils of Costa Rica. Geoderma 109, 141–160.

Pozzato, L., Cathalot, C., Berrached, C., Toussaint, F., Stetten, E., Caprais, J.-C., Pastor, L., Olu, K., Rabouille, C., 2017. Early diagenesis in the Congo deep-sea fan sediments

dominated by massive terrigenous deposits: Part I – Oxygen consumption and organic carbon mineralization using a micro-electrode approach. Deep Sea Research Part II: Topical Studies in Oceanography 142, 125–138.

Prahl, F.G., De Lange, G.J., Scholten, S., Cowie, G.L., 1997. A case of post-depositional aerobic degradation of terrestrial organic matter in turbidite deposits from the Madeira Abyssal Plain. Organic Geochemistry 27, 141–152.

Pruski, A.M., Buscail, R., Bourgeois, S., Vétion, G., Coston-Guarini, J., Rabouille, C., 2015. Biogeochemistry of fatty acids in a river-dominated Mediterranean ecosystem (Rhône River prodelta, Gulf of Lions, France): Origins and diagenesis. Organic Geochemistry 83–84, 227–240.

Pruski, A.M., Decker, C., Stetten, E., Vétion, G., Martinez, P., Charlier, K., Senyarich, C., Olu, K., 2017. Energy transfer in the Congo deep-sea fan: From terrestrially-derived organic matter to chemosynthetic food webs. Deep Sea Research Part II: Topical Studies in Oceanography 142, 197–218.

Pruski, A.M., Rzeznik-Orignac, J., Kerhervé, P., Vétion, G., Bourgeois, S., Péru, E., Brosset, P., Toussaint, F., Rabouille, C., 2021. Dynamic of organic matter and meiofaunal community on a river-dominated shelf (Rhône prodelta, NW Mediterranean Sea): Responses to river regime. Estuarine, Coastal and Shelf Science 253, 107274.

Rabouille, C., 2011. Congolobe cruise, Pourquoi pas ? R/V. doi:10.17600/11030170

Rabouille, C., Caprais, J.-C., Lansard, B., Crassous, P., Dedieu, K., Reyss, J.L., Khripounoff, A., 2009. Organic matter budget in the Southeast Atlantic continental margin close to the Congo Canyon: In situ measurements of sediment oxygen consumption. Deep Sea Research Part II: Topical Studies in Oceanography 56, 2223–2238.

Rabouille, C., Dennielou, B., Baudin, F., Raimonet, M., Droz, L., Khripounoff, A., Martinez, P., Mejanelle, L., Michalopoulos, P., Pastor, L., Pruski, A., Ragueneau, O., Reyss, J.-

L., Ruffine, L., Schnyder, J., Stetten, E., Taillefert, M., Tourolle, J., Olu, K., 2019. Carbon and silica megasink in deep-sea sediments of the Congo terminal lobes. Quaternary Science Reviews 222, 105854.

Rabouille, C., Olu, K., Baudin, F., Khripounoff, A., Dennielou, B., Arnaud-Haond, S., Babonneau, N., Bayle, C., Beckler, J., Bessette, S., Bombled, B., Bourgeois, S., Brandily, C., Caprais, J.C., Cathalot, C., Charlier, K., Corvaisier, R., Croguennec, C., Cruaud, P., Decker, C., Droz, L., Gayet, N., Godfroy, A., Hourdez, S., Le Bruchec, J., Le Saout, J., Lesaout, M., Lesongeur, F., Martinez, P., Mejanelle, L., Michalopoulos, P., Mouchel, O., Noel, P., Pastor, L., Picot, M., Pignet, P., Pozzato, L., Pruski, A.M., Rabiller, M., Raimonet, M., Ragueneau, O., Reyss, J.L., Rodier, P., Ruesch, B., Ruffine, L., Savignac, F., Senyarich, C., Schnyder, J., Sen, A., Stetten, E., Sun, M.Y., Taillefert, M., Teixeira, S., Tisnerat-Laborde, N., Toffin, L., Tourolle, J., Toussaint, F., Vétion, G., Jouanneau, J.M., Bez, M., 2017. The Congolobe project, a multidisciplinary study of Congo deep-sea fan lobe complex: Overview of methods, strategies, observations and sampling. Deep Sea Research Part II: Topical Studies in Oceanography 142, 7–24.

Remusat, L., Hatton, P.-J., Nico, P.S., Zeller, B., Kleber, M., Derrien, D., 2012. NanoSIMS study of organic matter associated with soil aggregates: Advantages, limitations, and combination with STXM. Environmental Science & Technology 46, 3943–3949.

Saliot, A., Parrish, C.C., Sadouni, N., Bouloubassi, I., Fillaux, J., Cauwet, G., 2002. Transport and fate of Danube Delta terrestrial organic matter in the Northwest Black Sea mixing zone. Marine Chemistry 79, 243–259.

Salmon, V., Derenne, S., Lallier-Vergès, E., Largeau, C., Beaudoin, B., 2000. Protection of organic matter by mineral matrix in a Cenomanian black shale. Organic Geochemistry 31, 463–474.

Santos, V., Billett, D.S.M., Rice, A.L., Wolff, G.A., 1994. Organic matter in deep-sea sediments from the Porcupine Abyssal Plain in the north-east Atlantic Ocean. I – Lipids. Deep Sea Research Part I: Oceanographic Research Papers 41, 787–810.

Savoye, B., Babonneau, N., Dennielou, B., Bez, M., 2009. Geological overview of the Angola-Congo margin, the Congo deep-sea fan and its submarine valleys. Deep-Sea Research Part II–Topical Studies in Oceanography 56, 2169–2182.

Savoye, B., Cochonat, P., Apprioual, R., Bain, O., Baltzer, A., Bellec, V., Beuzart, P., Bourillet, J.-F., Cagna, R., Cremer, M., Crusson, A., Dennielou, B., Diebler, D., Droz, L., Ennes, J.-C., Floch, G., Guiomar, M., Harmegnies, F., Kerbrat, R., Klein, B., Kuhn, H., Landuré, J.-Y., Lasnier, C., Le Drezen, E., Le Formal, J.-P., Lopez, M., Loubrieu, B., Marsset, T., Migeon, S., Normand, A., Nouzé, H., Ondréas, H., Pelleau, P., Saget, P., Séranne, M., Sibuet, J.-C., Tofani, R., Voisset, M., 2000. Structure et évolution récente de l'éventail turbiditique du Zaïre : premiers résultats scientifiques des missions d'exploration Zaïango1 & 2 (marge Congo–Angola). Comptes Rendus de l'Académie des Sciences - Series IIA - Earth and Planetary Science 331, 211–220.

Schefuß, E., Versteegh, G., Jansen, F., Sinninghe-Damsté, J., 2001. Marine and terrigenous lipids in Southeast Atlantic sediments (Leg 175) as paleoenvironmental indicators: initial results. In: Proceedings of the Ocean Drilling Program, Scientific Results. pp. 1–34.

Schefuß, E., Versteegh, G.J.M., Jansen, J.H.F., Sinninghe Damsté, J.S., 2004. Lipid biomarkers as major source and preservation indicators in SE Atlantic surface sediments. Deep Sea Research Part I: Oceanographic Research Papers 51, 1199–1228.

Schneider, R.R., Müller, P.J., Wefer, G., 1994. Late Quaternary paleoproductivity changes off the Congo deduced from stable carbon isotopes of planktonic foraminifera. Palaeogeography, Palaeoclimatology, Palaeoecology 110, 255–274.

Schnyder, J., Stetten, E., Baudin, F., Pruski, A.M., Martinez, P., 2017. Palynofacies reveal fresh terrestrial organic matter inputs in the terminal lobes of the Congo deep-sea fan. Deep-Sea Research Part II: Topical Studies in Oceanography 142, 91–108.

Schouten, S., Hopmans, E.C., Sinninghe Damsté, J.S., 2013. The organic geochemistry of glycerol dialkyl glycerol tetraether lipids: A review. Organic Geochemistry 54, 19–61.

Shi, W., Sun, M.-Y., Molina, M., Hodson, R.E., 2001. Variability in the distribution of lipid biomarkers and their molecular isotopic composition in Altamaha estuarine sediments: implications for the relative contribution of organic matter from various sources. Organic Geochemistry 32, 453–467.

Spencer, R.G.M., Hernes, P.J., Aufdenkampe, A.K., Baker, A., Gulliver, P., Stubbins, A., Aiken, G.R., Dyda, R.Y., Butler, K.D., Mwamba, V.L., Mangangu, A.M., Wabakanghanzi, J.N., Six, J., 2012. An initial investigation into the organic matter biogeochemistry of the Congo River. Geochimica et Cosmochimica Acta 84, 614–627.

Spencer, R.G.M., Stubbins, A., Hernes, P.J., Baker, A., Mopper, K., Aufdenkampe, A.K., Dyda, R.Y., Mwamba, V.L., Mangangu, A.M., Wabakanghanzi, J.N., Six, J., 2009. Photochemical degradation of dissolved organic matter and dissolved lignin phenols from the Congo River. Journal of Geophysical Research: Biogeosciences 114, doi:10.1029/2009JG000968

Spencer-Jones, C.L., Wagner, T., Dinga, B.J., Schefuß, E., Mann, P.J., Poulsen, J.R., Spencer, R.G.M., Wabakanghanzi, J.N., Talbot, H.M., 2015. Bacteriohopanepolyols in tropical soils and sediments from the Congo River catchment area. Organic Geochemistry 89–90, 1–13.

Stetten, E., Baudin, F., Reyss, J.-L., Martinez, P., Charlier, K., Schnyder, J., Rabouille, C., Dennielou, B., Coston-Guarini, J., Pruski, A.M., 2015. Organic matter characterization

and distribution in sediments of the terminal lobes of the Congo deep-sea fan: Evidence for the direct influence of the Congo River. Marine Geology 369, 182–195.

Sun, M.-Y., Wakeham, S.G., 1994. Molecular evidence for degradation and preservation of organic matter in the anoxic Black Sea Basin. Geochimica et Cosmochimica Acta 58, 3395–3406.

Sun, M.-Y., Zou, L., Dai, J., Ding, H., Culp, R.A., Scranton, M.I., 2004. Molecular carbon isotopic fractionation of algal lipids during decomposition in natural oxic and anoxic seawaters. Organic Geochemistry 35, 895–908.

Svetashev, V.I., 2022. Investigation of deep-sea ecosystems using marker fatty acids: sources of essential polyunsaturated fatty acids in abyssal megafauna. Marine Drugs 20, 17.

Talbot, H.M., Handley, L., Spencer-Jones, C.L., Dinga, B.J., Schefuß, E., Mann, P.J., Poulsen, J.R., Spencer, R.G.M., Wabakanghanzi, J.N., Wagner, T., 2014. Variability in aerobic methane oxidation over the past 1.2 Myrs recorded in microbial biomarker signatures from Congo fan sediments. Geochimica et Cosmochimica Acta 133, 387–401.

Talling, P., Baker, M., Pope, E., Jacinto, R.S., Heijnen, M., Hage, S., Simmons, S., Hasenhündl, M., Heerema, C., Ruffell, S., McGhee, C., Apprioual, R., Ferrant, A., Cartigny, M., Parsons, D., Clare, M., Tshimanga, R., Trigg, M., Cula, C., Faria, R., Gaillot, A., Bola, G., Wallace, D., Griffiths, A., Nunny, R., Urlaub, M., Peirce, C., Burnett, R., Neasham, J., Hilton, R., 2022. Flood and tides trigger longest measured sediment flow that accelerates for thousand kilometers into deep-sea. Nature Communications 13, 4193.

Teece, M.A., Fogel, M.L., Dollhopf, M.E., Nealson, K.H., 1999. Isotopic fractionation associated with biosynthesis of fatty acids by a marine bacterium under oxic and anoxic conditions. Organic Geochemistry 30, 1571–1579.

Treignier, C., Derenne, S., Saliot, A., 2006. Terrestrial and marine *n*-alcohol inputs and degradation processes relating to a sudden turbidity current in the Zaire canyon. Organic Geochemistry 37, 1170–1184.

Unger, D., Ittekkot, V., Schafer, P., Tiemann, J., 2005. Biogeochemistry of particulate organic matter from the Bay of Bengal as discernible from hydrolysable neutral carbohydrates and amino acids. Marine Chemistry 96, 155–184.

Van Bennekom, A.J., Berger, G.W., 1984. Hydrography and silica budget of the Angola Basin. Netherlands Journal of Sea Research 17, 149–200.

Van Vleet, E.S., Quinn, J.G., 1979. Diagenesis of marine lipids in ocean sediments. Deep Sea Research Part A. Oceanographic Research Papers 26, 1225–1236.

Vangriesheim, A., Pierre, C., Aminot, A., Metzl, N., Baurand, F., Caprais, J.-C., 2009. The influence of Congo River discharges in the surface and deep layers of the Gulf of Guinea. Deep Sea Research Part II: Topical Studies in Oceanography 56, 2183–2196.

Volkman, J.K., Barrett, S.M., Blackburn, S.I., Mansour, M.P., Sikes, E.L., Gelin, F., 1998. Microalgal biomarkers: A review of recent research developments. Organic Geochemistry 29, 1163–1179.

Volkman, J.K., Jeffrey, S.W., Nichols, P.D., Rogers, G.I., Garland, C.D., 1989. Fatty acid and lipid composition of 10 species of microalgae used in mariculture. Journal of Experimental Marine Biology and Ecology 128, 219–240.

Wakeham, S.G., Canuel, E.A., 2006. Degradation and Preservation of Organic Matter in Marine Sediments. In: Volkman, J.K. (Ed.), Marine Organic Matter: Biomarkers, Isotopes and DNA, The Handbook of Environmental Chemistry. Springer, Berlin, Heidelberg, pp. 295–321.

Wakeham, S.G., Lee, C., Hedges, J.I., Hernes, P.J., Peterson, M.L., 1997a. Molecular indicators of diagenetic status in marine organic matter. Geochimica et Cosmochimica Acta 61, 5363–5369.

Wakeham, S.G., Hedges, J.I., Lee, C., Peterson, M.L., Hernes, P.J., 1997b. Compositions and transport of lipid biomarkers through the water column and surficial sediments of the equatorial Pacific Ocean. Deep Sea Research Part II: Topical Studies in Oceanography, A JGFOS Process Study in the Equatorial Pacific 44, 2131–2162.

Wakeham, S.G., Canuel, E.A., Lerberg, E.J., Mason, P., Sampere, T.P., Bianchi, T.S., 2009. Partitioning of organic matter in continental margin sediments among density fractions. Marine Chemistry 115, 211–225.

Wakeham, S.G., Turich, C., Schubotz, F., Podlaska, A., Li, X.N., Varela, R., Astor, Y., Sáenz, J.P., Rush, D., Sinninghe Damsté, J.S., Summons, R.E., Scranton, M.I., Taylor, G.T., Hinrichs, K.-U., 2012. Biomarkers, chemistry and microbiology show chemoautotrophy in a multilayer chemocline in the Cariaco Basin. Deep Sea Research Part I: Oceanographic Research Papers 63, 133–156.

Wang, Z., Liu, W., 2012. Carbon chain length distribution in n-alkyl lipids: A process for evaluating source inputs to Lake Qinghai. Organic Geochemistry 50, 36–43.

Wang, X., Sun, M., Lil, A., 2008. Contrasting chemical and isotopic compositions of organic matter in Changjiang (Yangtze river) estuarine and East China Sea shelf sediments. Journal of Oceanography 64, 311–321.

Wang, X.-C., Druffel, E.R.M., 2001. Radiocarbon and stable carbon isotope compositions of organic compound classes in sediments from the NE Pacific and Southern Oceans. Marine Chemistry 73, 65–81.

Wang, X.-C., Druffel, E.R.M., Griffin, S., Lee, C., Kashgarian, M., 1998. Radiocarbon studies of organic compound classes in plankton and sediment of the northeastern Pacific Ocean. Geochimica et Cosmochimica Acta 62, 1365–1378.

Weijers, J.W.H., Schouten, S., Spaargaren, O.C., Sinninghe Damsté, J.S., 2006. Occurrence and distribution of tetraether membrane lipids in soils: Implications for the use of the TEX86 proxy and the BIT index. Organic Geochemistry 37, 1680–1693.

Weijers, J.W.H., Schouten, S., Schefuß, E., Schneider, R.R., Sinninghe Damsté, J.S., 2009. Disentangling marine, soil and plant organic carbon contributions to continental margin sediments: A multi-proxy approach in a 20,000 year sediment record from the Congo deep-sea fan. Geochimica et Cosmochimica Acta 73, 119–132.

Weijers, J.W.H., Schefuß, E., Kim, J.-H., Sinninghe Damsté, J.S., Schouten, S., 2014. Constraints on the sources of branched tetraether membrane lipids in distal marine sediments. Organic Geochemistry 72, 14–22.

Wenzhöfer, F., Glud, R.N., 2002. Benthic carbon mineralization in the Atlantic: a synthesis based on in situ data from the last decade. Deep Sea Research Part I: Oceanographic Research Papers 49, 1255–1279.

Wiesenberg, G.L.B., Dorodnikov, M., Kuzyakov, Y., 2010. Source determination of lipids in bulk soil and soil density fractions after four years of wheat cropping. Geoderma 156, 267–277.

Wilson, T.R.S., Thomson, J., Colley, S., Hydes, D.J., Higgs, N.C., Sørensen, J., 1985. Early organic diagenesis: The significance of progressive subsurface oxidation fronts in pelagic sediments. Geochimica et Cosmochimica Acta 49, 811–822.

Figure captions

Fig. 1. (A) General bathymetric map showing the Congo deep-sea fan with its active channel, and (B) a EM12 Backscatter sonar image of the terminal part of the Congo deep-sea fan with location of the sampling sites: A, E, C and B are located in the recent lobe complex; F is located in an abandoned lobe complex. The orange box in A indicates the study area and the red box the location of the Malebo Pool at Kinshasa, whereas the dotted orange line in B shows the limit of the terminal lobe complex. Coordinates of sampling sites are provided in Supplementary Table S1.

Fig. 2. Fatty acid composition of Congo River sediments collected on land (Malebo Pool) and marine suspended POM recovered in surface waters above the terminal lobe complex. Results are expressed in percent of total fatty acids (N = 6 for Congo River sediments and N = 5 for suspended POM). The bold line represents median value, the box is the mid-spread (including the first and third quartiles), and the whiskers are the minimum and maximum values. Data beyond the end of the whiskers are outliers.

Fig. 3. OC-normalised fatty acid concentrations, cumulative biomarker contributions, and OC content (%) in the surface sediments from the terminal lobe complex of the Congo deep-sea fan (layer 0–0.5 cm) and on land at the Malebo Pool (layer 0–5 cm).

Fig. 4. Downcore evolution of bulk $\delta^{13}C$, fatty acid subgroup contributions and proportion of terrestrial phytoclasts in the sediment cores collected in (A) the channel at site C and (B) the abandoned site E. Values were plotted at the mid depth of the layer (11 layers for fatty acids and $\delta^{13}C$ values, 9 for palynofacies counts). Long chain fatty acids = LCFA, polyunsaturated fatty acids = PUFA, bacterial fatty acids = BAFA and monounsaturated fatty acids = MUFA. Palynofacies data are from Schnyder et al. (2017). The yellow area indicates the oxygen

penetration depth (OPD; Pozzato et al., 2017). Note the similar vertical distribution of LCFA and terrestrial phytoclasts at site E.

Fig. 5. Fatty acid-based hierarchical cluster analysis of sediments from the terminal lobe complex of the Congo deep-sea fan (A) and average composition of the four clusters (B). Bray-Curtis dissimilarity index and Ward's minimum variance linkage method were used for clustering. Average composition for each cluster is expressed as percentages of total fatty acids. Code for sediment samples is: AL (site A levee), AC (site A channel), CL (site C levee), CC (site C channel), B (site B), F (site F), and E (site E) followed by sediment layers from 0 for surface layer (0–0.5 cm) to 10 for the deepest sediment layer (19–22 cm).

Fig. 6. Non-metric multidimensional scaling (nMDS) ordination plot assessing the relationship between sites, sampling depths, fatty acid biomarkers, and sediment properties in the terminal lobe area of the Congo deep-sea fan (stress = 0.116). Code for sediment samples is: AL (site A levee), AC (site A channel), CL (site C levee), CC (site C channel), B (site B), and F (site F) followed by sediment layers from 0 for surface layer (0–0.5 cm) to 10 for the deepest sediment layer (19–22 cm). The distance between samples indicates similarity of the fatty acid composition, i.e., the closer = the more similar. Environmental factors were fitted in the ordination plot as vectors, whereby the arrow indicates the direction of the increasing gradient of the environmental variable and the length of the arrow is proportional to the correlation coefficient between the variable and the nMDS ordination.

Fig. 7. Conceptual scheme summarising the principal outcomes of this study. Processes affecting marine and terrestrial organic matter during transit and after deposition in the

terminal lobe area of the Congo deep-sea fan are presented. The blue box presents the different depositional scenarios in the recent and abandoned lobe complexes.

Table 1. Principal descriptors used in this study with their interpretation.

Descriptors	Feature	Main diagnostic information	References
C/N	Source/Quality	Marine derived OM (6–9), Soil derived OM (8–20) and higher plants (>20)	1–3
$\delta^{13}C$	Source	POM Gulf of Guinea (–21‰), POM Congo River (–26.7 ± 0.4‰), Savannah soils (–26‰), C_3 vascular plant from the Angola (–28.0 ± 1.8‰) and C_4 vegetation (–13.6‰)	4–7
DI	Quality	Diagenetic alteration of OM with DI values ranging from −2.2 extensively degraded sediments to 1.5 for fresh algae	8
OI	Quality	Oxygen content of the OM	9
BIT index	Source	Proxy of soil OM with values of 0.91 ± 0.14 for Congo soils and 0.04 for marine OM	10,11
Fatty acids			
SCFA	Source	Mixed origin, but shorter chains predominate in phytoplankton	12,13
LCFA	Source	Terrestrial higher plants, macrodetritus	14
PUFA: 18:2ω6 and 18:3ω3	Source	Terrestrial higher plants (>2.5%)	16,17
PUFA: all except 18:2ω6 and 18:3ω3	Source/Quality	Phytoplankton with $C_{20:5\omega3}$ specific for diatoms and $C_{22:6\omega3}$ specific for dinoflagellates	12,18
MUFA	Source	Mixed origin with $C_{16:1\omega7}$ common in diatoms and bacteria and $C_{18:1\omega7}$ abundant in bacteria	12,13
BAFA	Source	Bacterial sources: Includes odd saturated ($C_{15:0}$, $C_{17:0}$), branched (iC_{15}, iC_{17}, aiC_{15}, aiC_{17}), and ß-hydroxylated fatty acids	13
UI	Quality	OM degradation (<70 old detrital matter)	19
CPI	Source/Quality	Expected to decrease with ongoing degradation (in soils <10 degraded OM)	20
ACL	Source/Quality	Expected to increase with ongoing degradation, higher in plant tissues than in microorganisms or aquatic plants	21,22

1: Moloney and Field (1991), 2: Hedges and Oades (1997), 3: Meyers (1997), 4: Badewien et al. (2015), 5: Delègue et al. (2001), 6: Fischer et al. (1998), 7: Powers and Schlesinger (2002), 8: Dauwe et al. (1999), 9: Espitalié et al. (1985), 10: Weijers et al. (2006), 11: Schouten et al. (2013), 12: Dunstan et al. (1994), 13: Bianchi and Canuel (2011), 14: Eglinton and Hamilton (1967), 15: Volkman et al. (1989), 16: Budge et al. (2001), 17: Pruski et al. (2015), 18: Volkman et al. (1998), 19: Claustre et al. (1992), 20: Angst et al. (2016), 21: Wiesenberg et al. (2010), 22: Wang and Liu (2012).

Table 2. Geochemical and sedimentological properties of the sediments from the terminal lobe complex of the Congo deep-sea fan. Organic carbon (OC), C/N (molar ratio), isotopic value of stable carbon ($\delta^{13}C$), isotopic value of stable nitrogen ($\delta^{15}N$), oxygen index (OI), Dauwe's degradation index (DI), and percentages of clay, silt and sand. The mean, lowest and highest values measured for each core are given. N = 4, except for C channel and E abandoned where N = 11. Data are from Stetten et al. (2015), except for OI (Baudin et al., 2017b) and DI (Pruski et al., 2017).

Site	OC %			C/N molar			$\delta^{13}C$ ‰			$\delta^{15}N$ ‰			OI mg CO_2/g OC			DI			Clay %			Silt %			Sand %		
	mean	min	max	mean	min	max	mean	min	max	mean	min	max	mean	min	max	mean	min	max	mean	min	max	mean	min	max	mean	min	max
A channel	3.0	2.7	3.7	16.9	15.3	18.2	–26.5	–26.8	–26.1	5.4	4.7	6.2	280.5	269	295	–0.2	–0.42	–0.08	19.4	14.8	22.4	75.6	73.2	77.9	4.8	2.5	7.3
A levee	3.0	2.7	3.5	16.6	14.5	19.9	–26.2	–26.7	–25.7	5.5	4.6	5.9	301.8	262	324	–0.1	–0.40	0.18	17.0	12.5	20.1	73.7	70.2	77.1	9.4	4.5	15.6
F levee	2.8	2.4	3.4	15.7	14.0	16.7	–25.9	–26.3	–25.2	5.4	5.2	5.6	288.3	278	305	–0.2	–0.32	0.15	20.1	15.5	22.0	75.7	73.8	78.1	4.3	0.8	8.3
C channel	3.8	3.2	4.1	15.6	14.7	17.1	–26.9	–27.1	–26.5	5.3	4.7	5.8	275.0	258	292	0.1	–0.41	0.61	23.0	20.0	26.0	71.2	69.2	73.5	5.6	2.1	10.4
C levee	2.9	2.2	3.4	15.0	13.9	15.8	–26.4	–26.6	–26.1	4.9	4.7	5.0	304.3	276	323	–0.1	–0.36	0.22	26.6	25.4	28.1	72.4	70.7	74.2	0.9	0.3	2.7
B	2.6	2.2	2.9	17.4	14.1	22.5	–25.9	–26.4	–25.3	5.3	4.8	5.9	265.0	244	295	16.5	–0.39	0.15	76.3	14.8	18.9	7.1	74.5	78.5	–0.1	5.7	9.0
E abandoned 0–7cm	0.8	0.7	0.9	11.4	11.0	11.7	–23.2	–23.9	–22.8	7.8	7.1	8.2	499.7	447	609	–1.1	–1.39	–0.87	24.4	17.7	30.9	71.7	68.2	74.2	3.6	0.9	8.8
E abandoned 7–22cm	1.9	1.2	2.8	14.0	12.3	15.9	–25.4	–26.9	–24.1	6.4	6.3	6.6	231.0	200	270	–0.1	–0.52	0.24	26.6	23.9	31.1	71.1	67.3	73.8	2.3	1.6	2.7

Table 3. BIT index values calculated for surface and deep horizons of sediments sampled from the terminal lobe complex. 0–1 cm layers were obtained by pooling the 0–0.5 cm and 0.5–1 cm horizons.

	Present-day active lobe complex						Northern lobe complex
Sediment layer	A channel	A levee	F levee	C channel	C levee	B	E abandoned
0–1 cm	0.75	0.76	0.76	0.83	0.81	0.78	0.48
19–22 cm	0.84	0.84	0.83	0.84	0.84	0.82	0.76

Table 4. Environmental fitting significance and correlation with nMDS axes of the main geochemical properties. Significant variables are indicated in bold, * $p < 0.05$, ** $p < 0.01$, ** $p < 0.001$.

Parameter	nMDS1	nMDS2	r^2	p value	
UI	0.98	0.22	0.89	0.001	***
CPI	–0.15	0.99	0.78	0.001	***
ACL	–0.59	0.81	0.63	0.001	***
$\delta^{13}C$	–0.98	–0.19	0.59	0.001	***
DI	0.96	0.27	0.47	0.001	***
OC	1	0.02	0.42	0.001	***
C/N	0.13	0.99	0.4	0.002	**
Silt	–0.62	0.78	0.24	0.019	*
Clay	0.55	–0.84	0.19	0.047	*
$\delta^{15}N$	–0.33	–0.94	0.17	0.073	
OI	–0.31	0.95	0.11	0.199	
Sand	–0.32	0.95	0.03	0.675	

Table 5. Preservation factors (Pf in %) for fatty acids in turbidites from the terminal lobe area of the Congo deep-sea fan. Values are means for the specific compound class and, between brackets, minimal and maximal Pf within the compound class.

	SCFA	LCFA	MUFA	PUFA*	BAFA
Site A channel	95.1 (73.9–144)	86.6 (69.7–119)	126 (105–152)	211	157 (125–332)
Site A levee	75.9 (54.7–102)	75.6 (49.8–151)	60.4 (38.7–99.2)	78.8	90.8 (70.0–103)
Site C channel	70.2 (55.8–98.1)	114.0 (82.2–131)	22.6 (18.5–28.5)	10.4	72.1 (53.8–105)
Site C levee	95.8 (83.8–124)	66.5 (63.6–71.1)	38.4 (33.4–46.6)	42.7	126 (94.1–192)
Site F	96.6 (85.4–122)	137.8 (98.2–168)	32.6 (16.8–46.5)	0.0	145 (74.8–292)
Site B	66.6 (56.2–89.5)	75.5 (61.7–84.2)	15.4 (10.2–25.5)	0.0	80.8 (55.5–113)

Preservation factors were calculated according to Hoefs et al. (2002), but only considered the first unoxidised layer (3–5 cm), as the layer 19–22 cm tended to be coarser which affected the OM content.

$\mathrm{Pf} = \frac{[C_{0-0.5\mathrm{cm}}]}{[C_{3-5\mathrm{cm}}]} \times 100$ where Pf: preservation factor and [C]: concentration of specific biomarker in µg g^{-1} dry sediments.

Pf values below 100% are signs of oxic degradation, whereas values above 100% are indicative of a post-depositional enrichment.

* Due to low concentrations Pf values were calculated on the sum of all PUFAs.

Declaration of interests

☐ The authors declare that they have no known competing financial interests or personal relationships that could have appeared to influence the work reported in this paper.

☒ The authors declare the following financial interests/personal relationships which may be considered as potential competing interests:

Pruski Audrey reports financial support was provided by French National Research Agency.

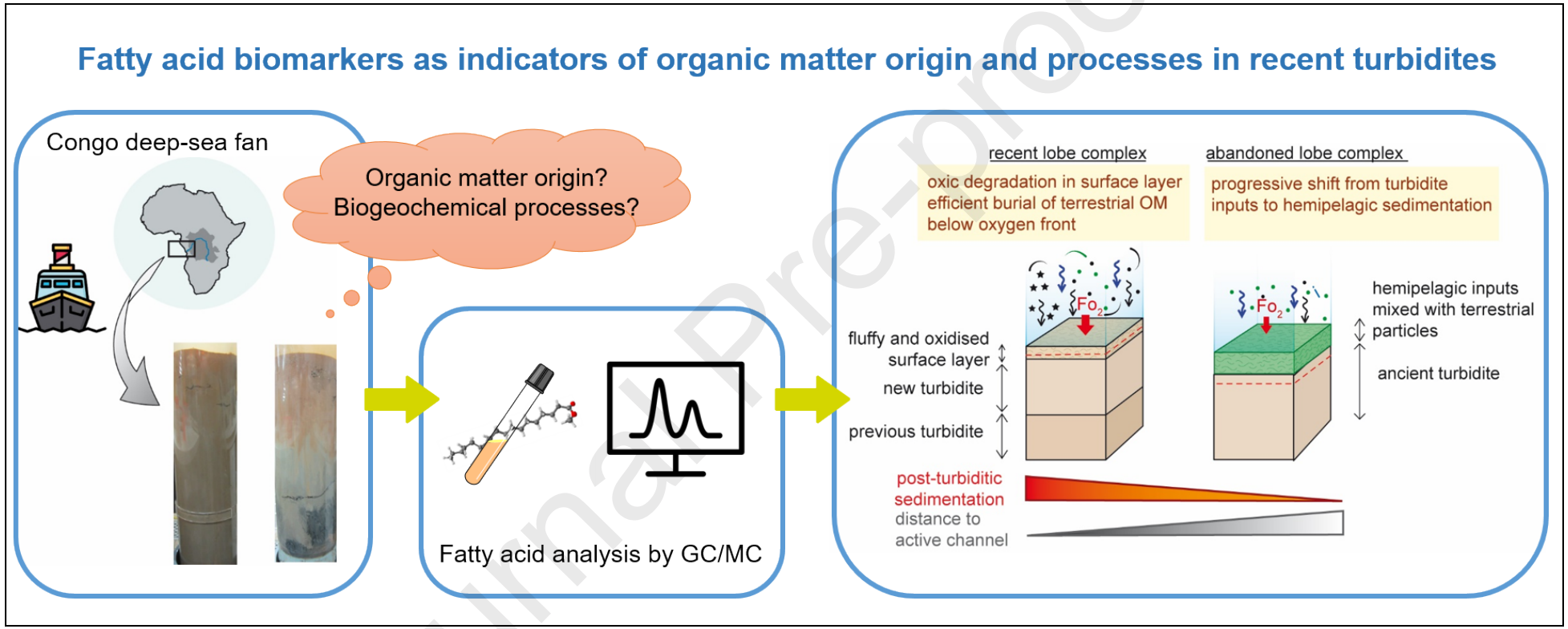

Fatty acids in Congo lobe sediments are mainly of terrestrial origin

Soil OM is distributed homogenously and plant debris heterogeneously

Small amounts of biomarkers from phytoplankton reach the terminal lobe complex

Oxic degradation is limited to the topmost surface sediments

Long chain fatty acids are preserved in turbidite deposits over millennia

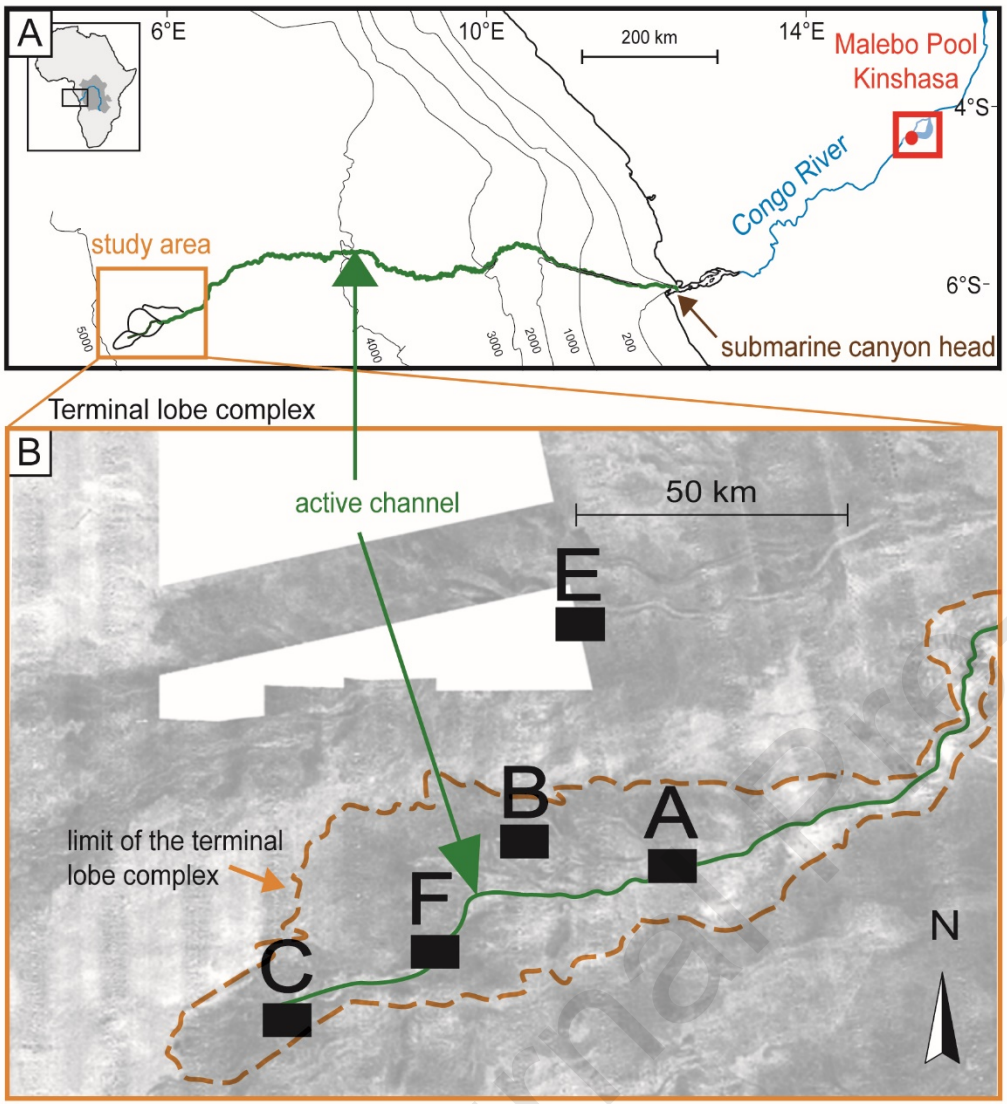

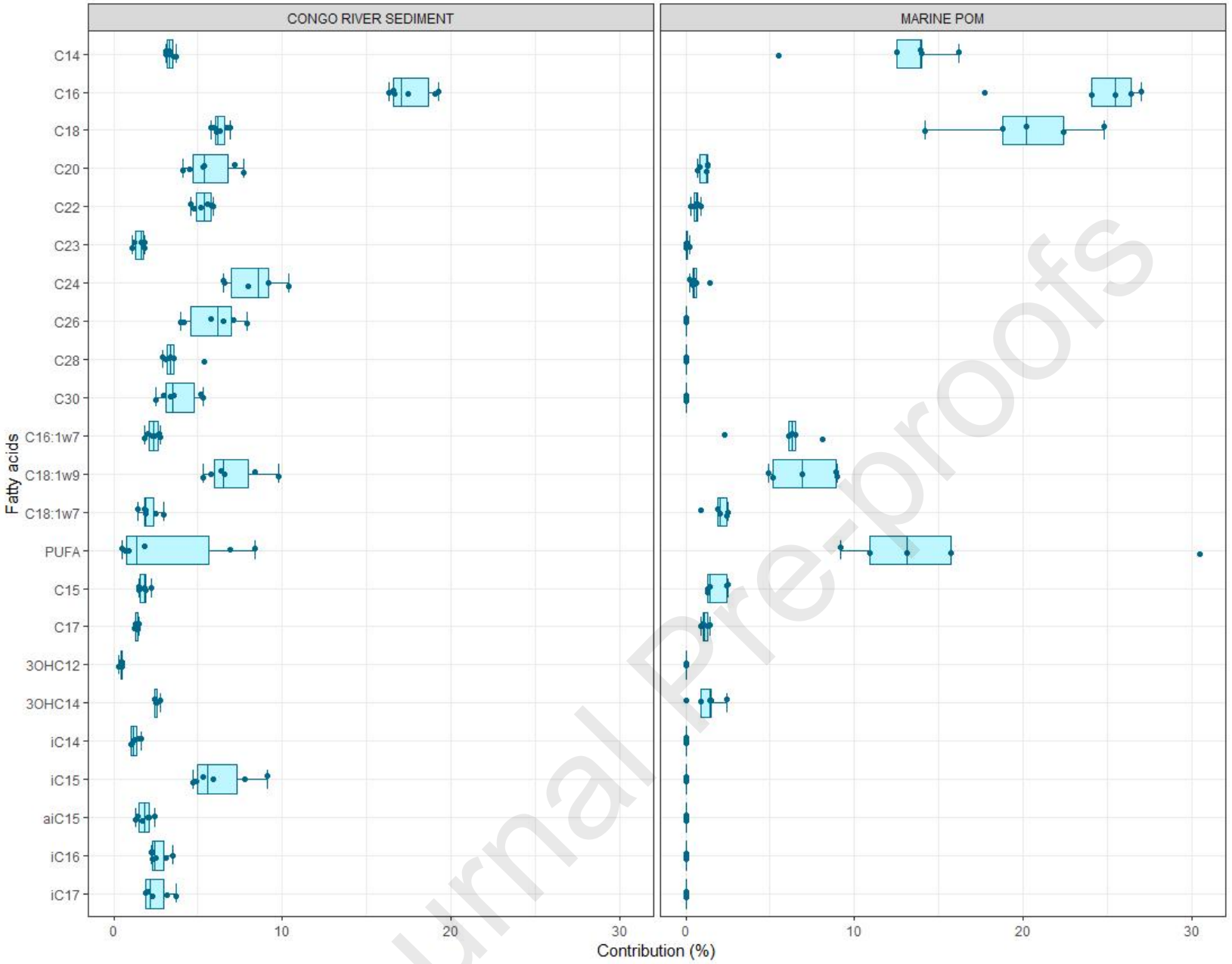

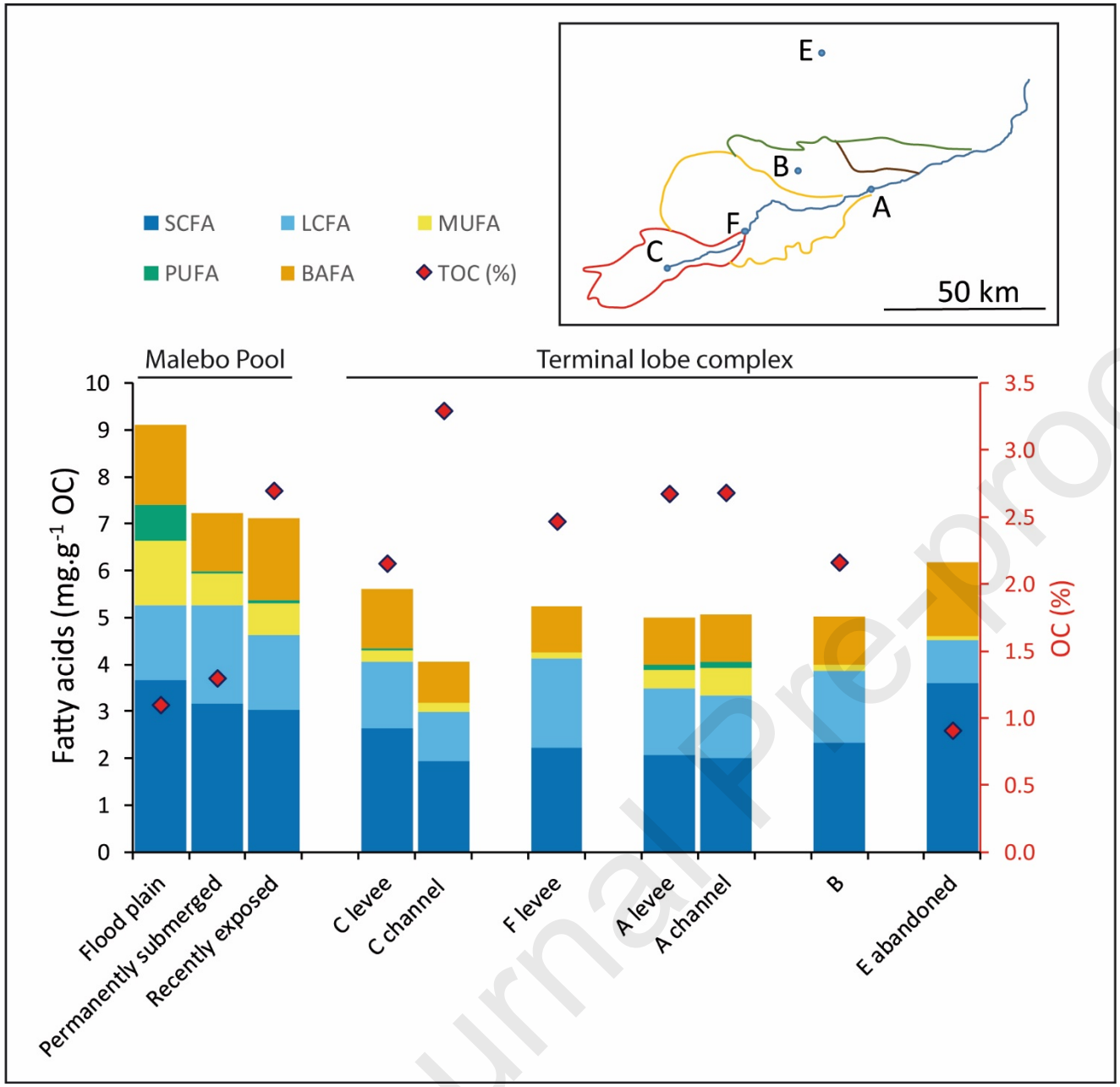

A- SITE C

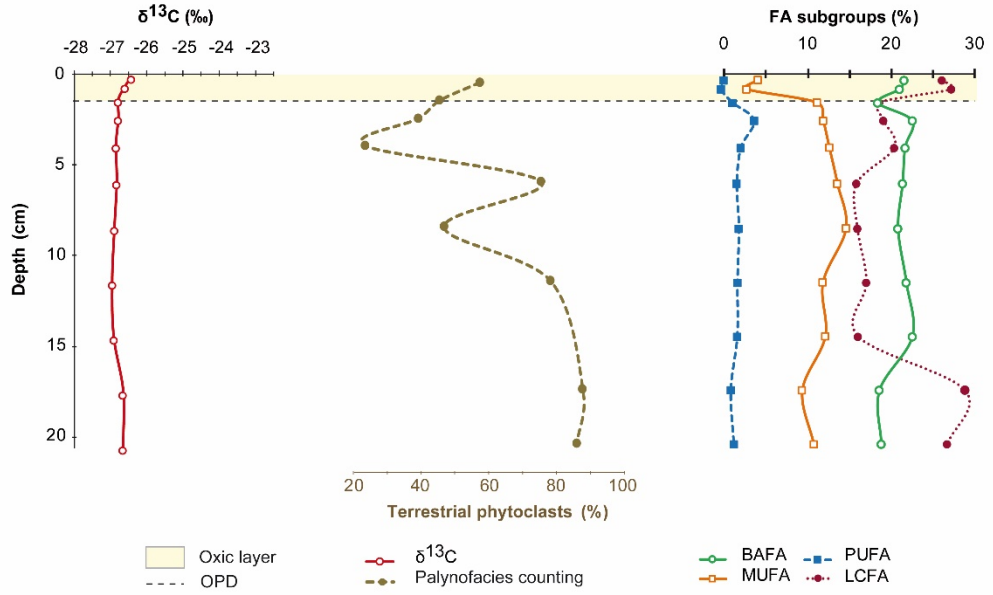

B- SITE E

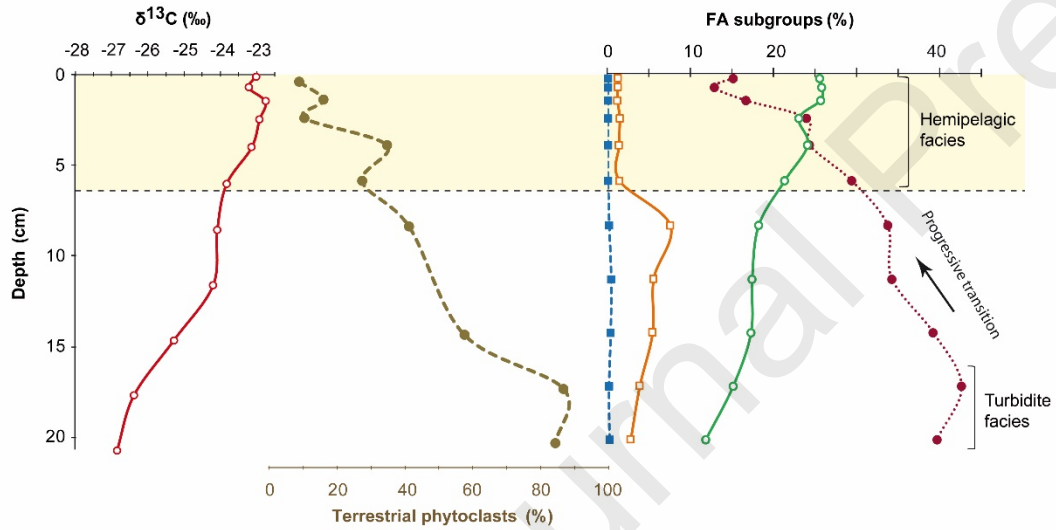

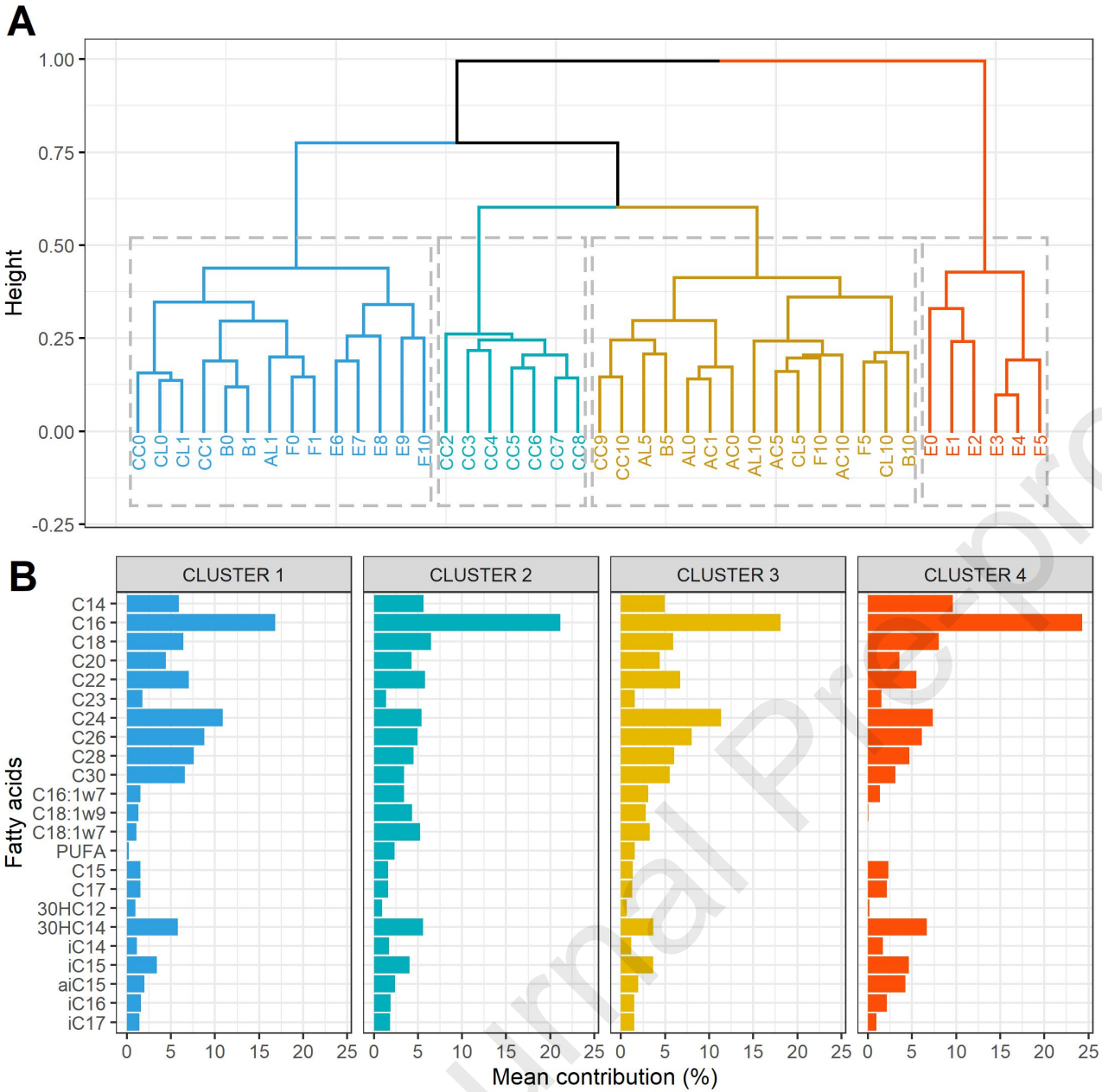

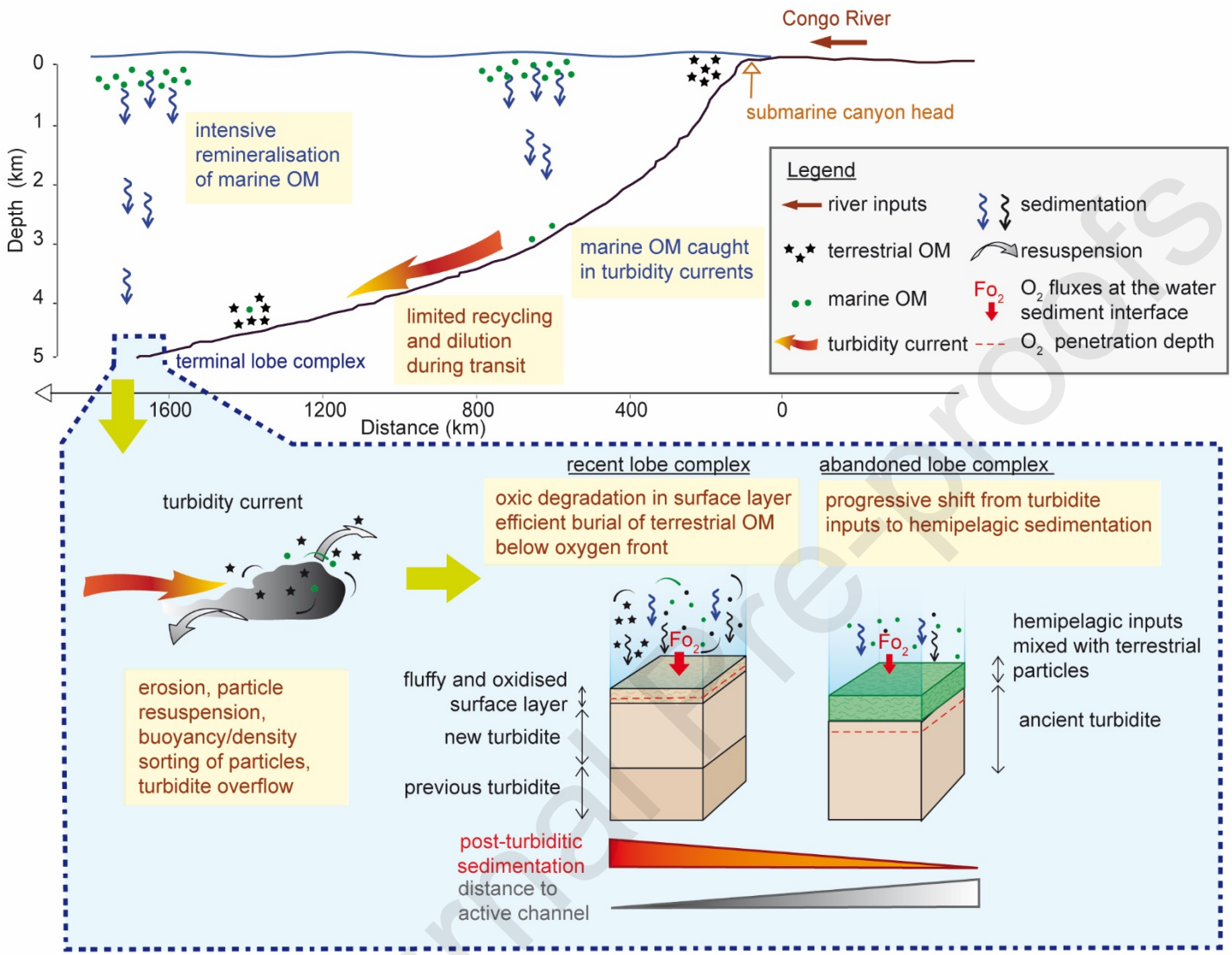
Congo River
submarine canyon head
intensive remineralisation of marine OM
marine OM caught in turbidity currents
limited recycling and dilution during transit
terminal lobe complex
Depth (km)
0
1
2
3
4
5
1600
1200
800
400
0
Distance (km)
Legend
river inputs
sedimentation
terrestrial OM
resuspension
marine OM
Fo2
O2 fluxes at the water sediment interface
turbidity current
O2 penetration depth
turbidity current
erosion, particle resuspension, buoyancy/density sorting of particles, turbidite overflow
recent lobe complex
oxic degradation in surface layer efficient burial of terrestrial OM below oxygen front
abandoned lobe complex
progressive shift from turbidite inputs to hemipelagic sedimentation
fluffy and oxidised surface layer
new turbidite
previous turbidite
Fo2
Fo2
hemipelagic inputs mixed with terrestrial particles
ancient turbidite
post-turbiditic sedimentation
distance to active channel